# Ionospheric monitoring and short term forecasting at middle latitudes during solar extreme events

**Anna Belehaki**

**Institute for Space Applications and Remote Sensing**

**National Observatory of Athens**

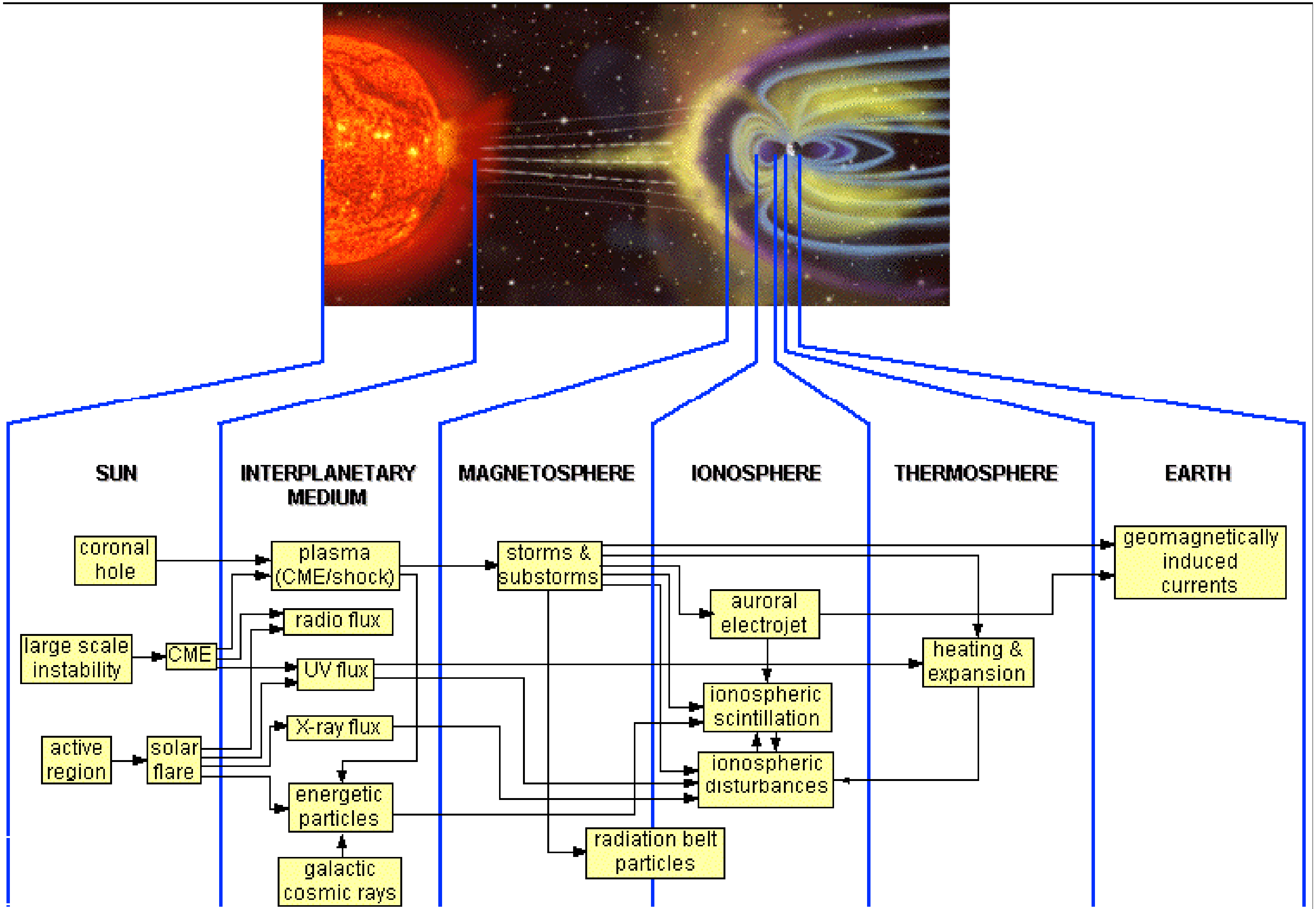


Main physical processes that act on space weather (Lathuillère et al., 2002)

# Effects at Earth of Space Weather Events

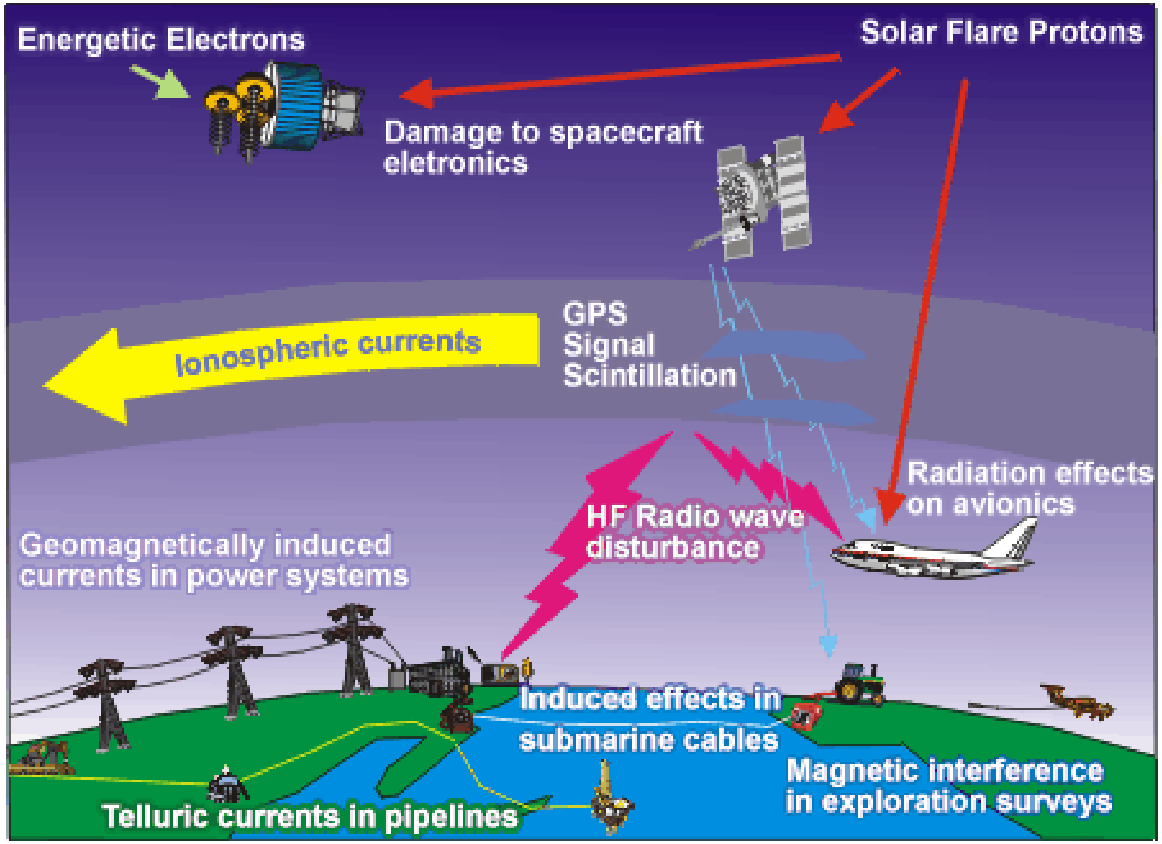


*From Natural Resources Canada*

Satellite Damage and Difficulties

Communications Black Outs and Radio Difficulties

Flow of Currents on Pipelines

Electric Power Problems

Confused Birds

# Effects on radio communication

1. Polar Cap Absorption event: Short wave radio waves absorption at HF
2. Short Wave Fadeout: Absorption of short wave radio waves (in the HF range) by the increased particles in the low altitude ionosphere causing a complete black out of radio communications
3. Signal scintillations: Some ionospheric layers are filled with small-scale irregular density structures.
4. Ionospheric Storms: Bands of enhanced density appear at high latitudes due to the high velocity particles that precipitate into the atmosphere, smashing into the neutral atmospheric gases and knocking electrons free. The same particles produce the auroral lights.

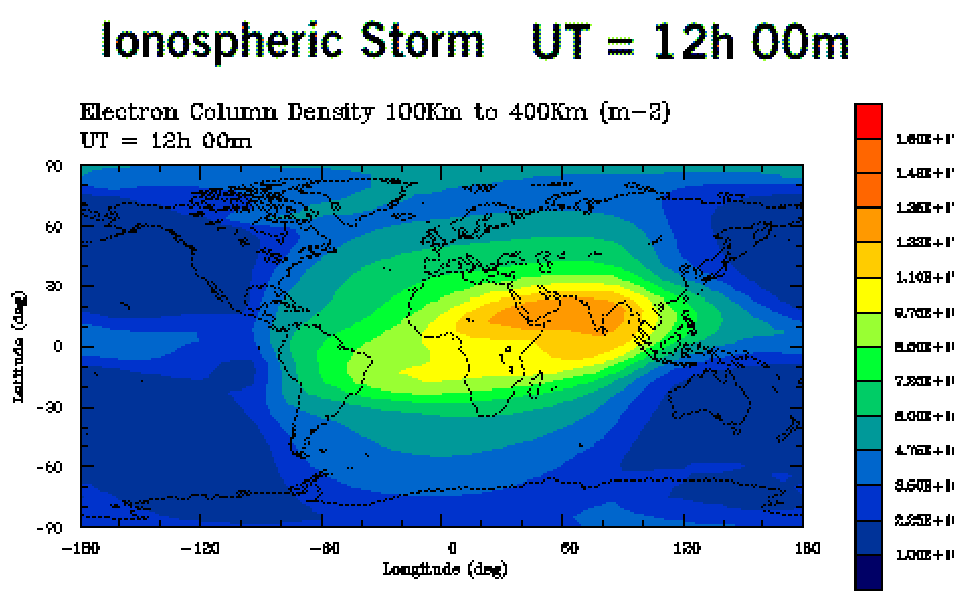

# Advanced specifications of modern ionosondes

- automatic scaling of ionograms
- determination of the ionospheric structure in real-time
- reconstruction of electron density profile in real-time
- calculation of the Ionospheric Total Electron Content (ITEC)
- determination of ionospheric motions and drift velocities

# Real-time electron density profiles calculation

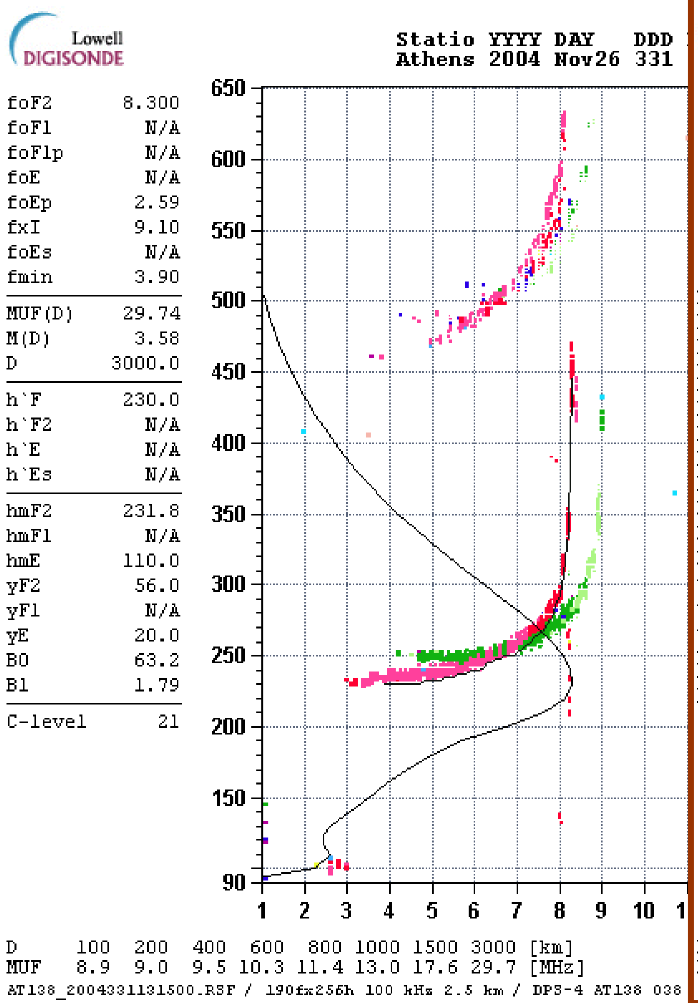


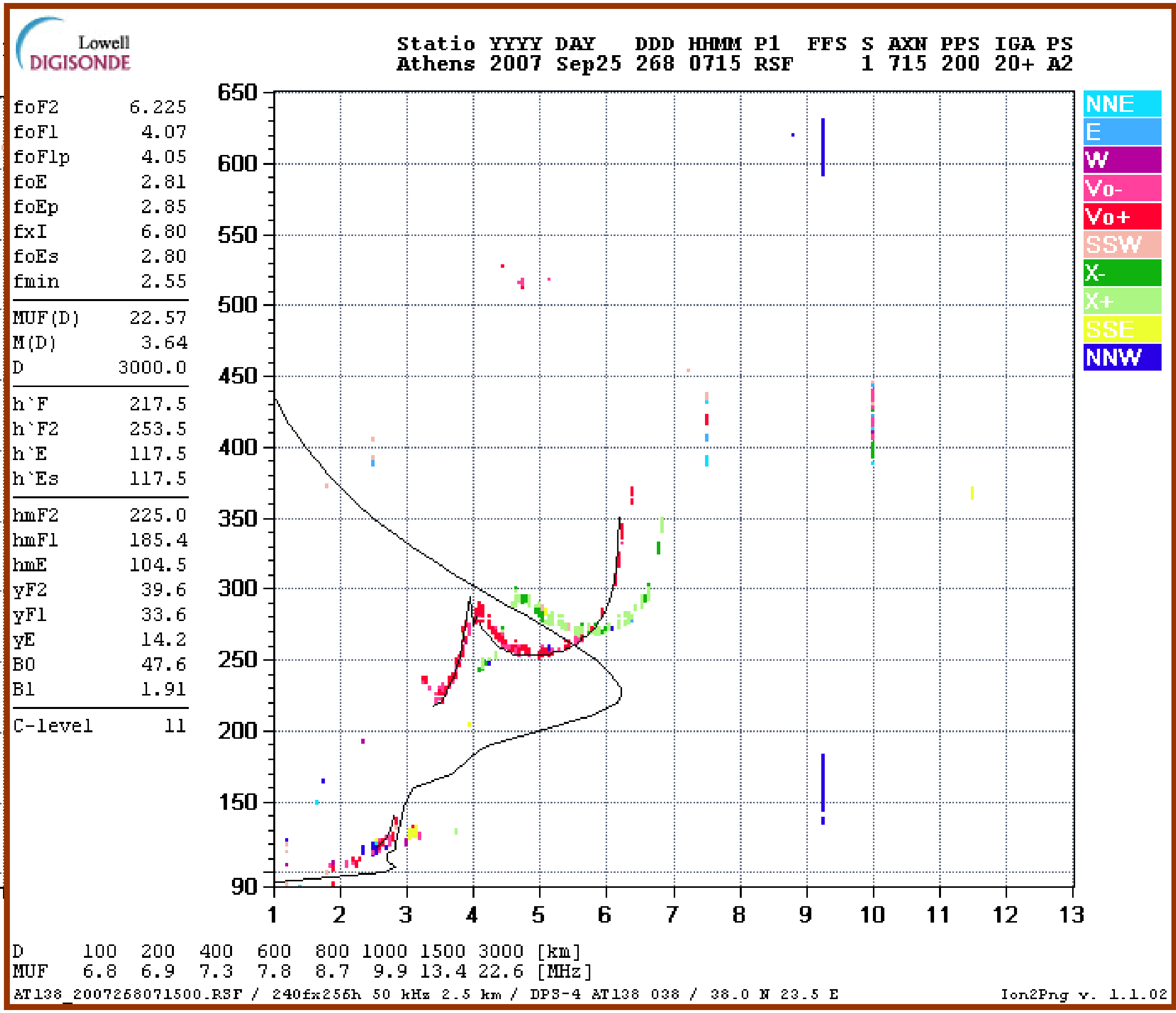

# Real-time determination of sporadic E layers casing total F-layer blanketing

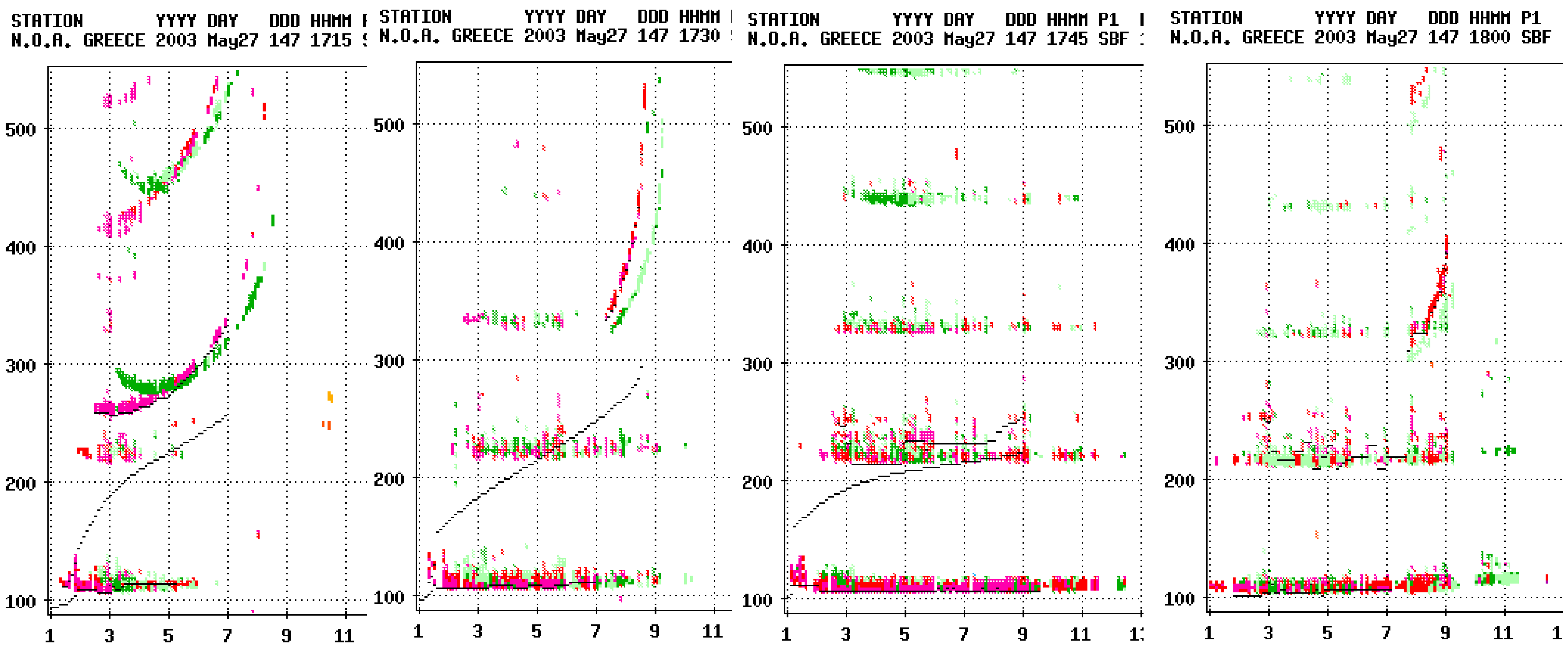


17:15UT 17:30UT 17:45UT 18:00UT

# Real-time determination of Patchy sporadic E-layers accompanied by mid-latitude spread F

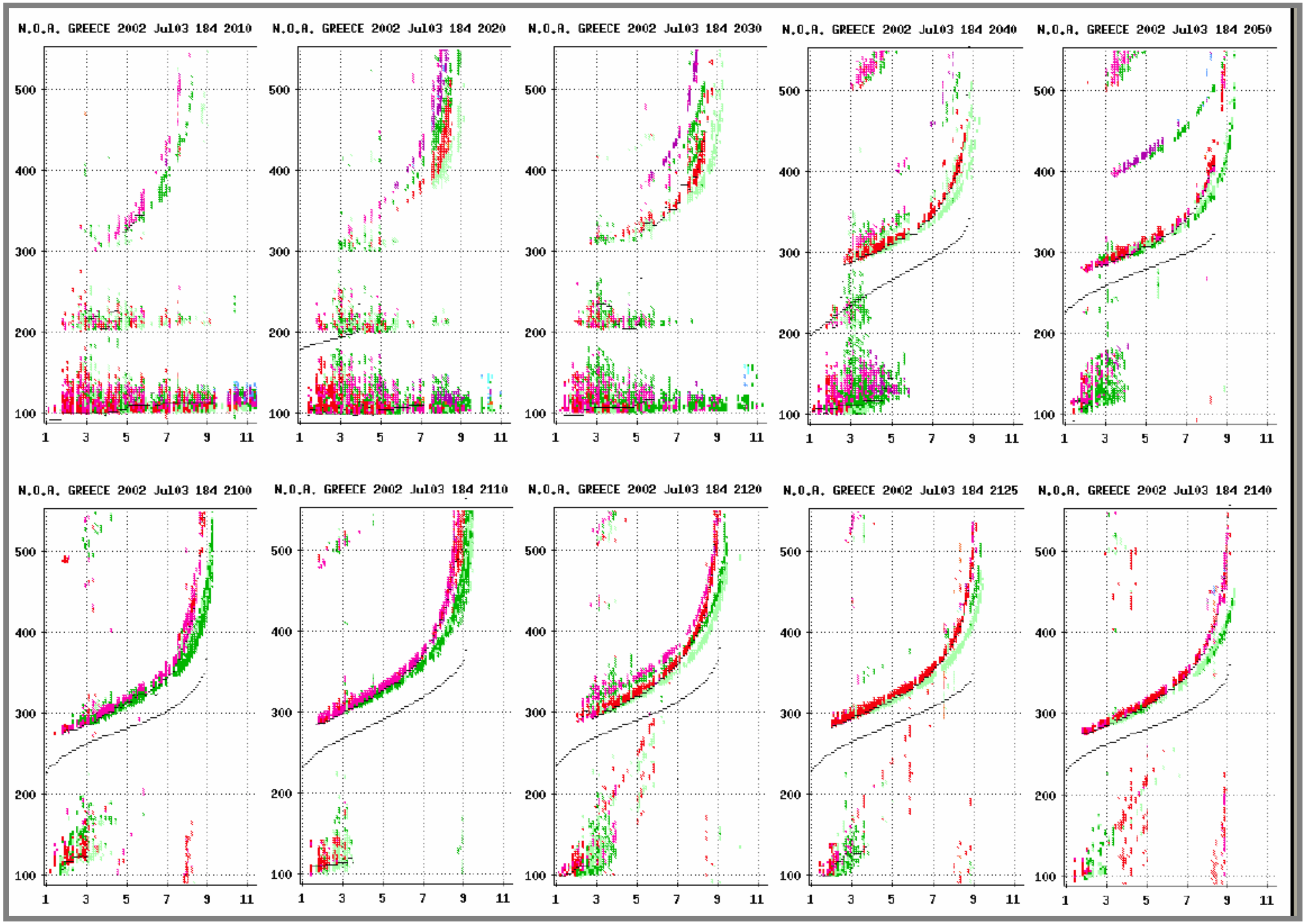

# Ionogram auto-scaling performance during geomagnetic storms

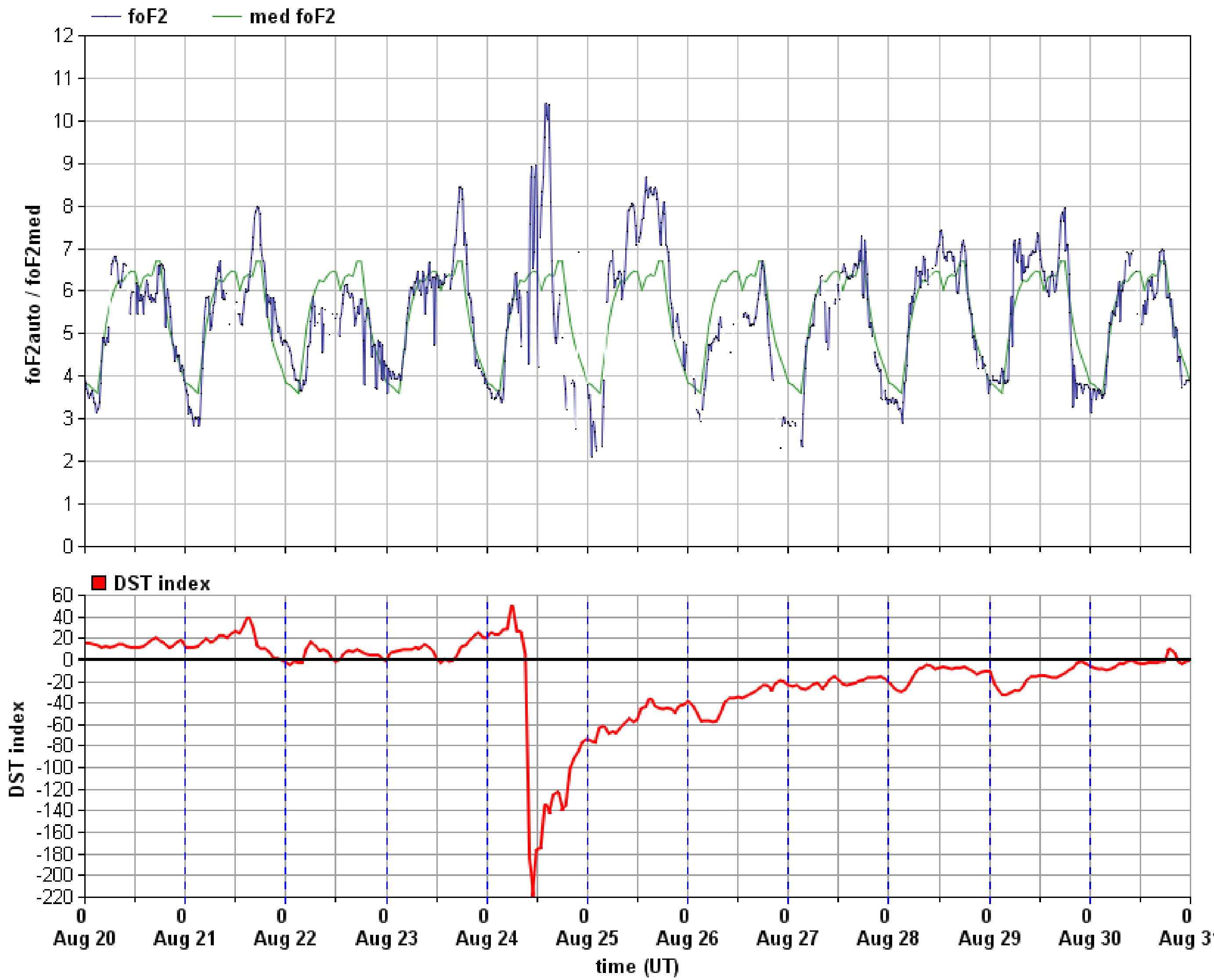

# SEE 2007

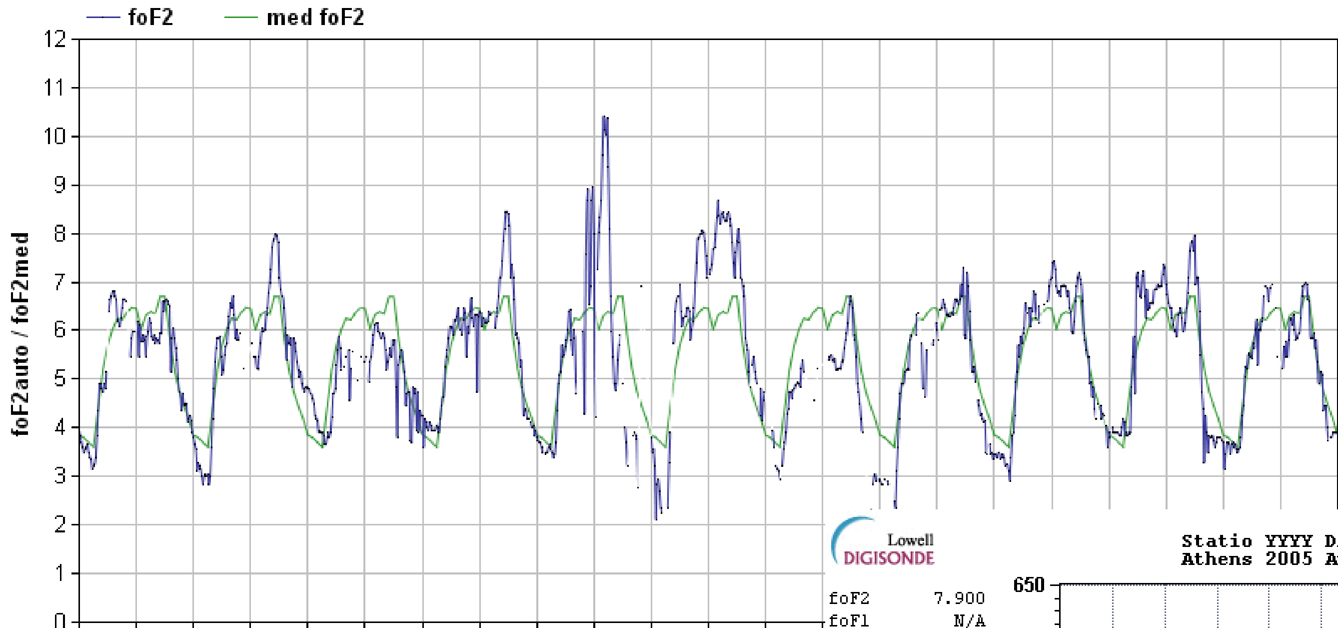

foF2
med foF2
foF2auto / foF2med


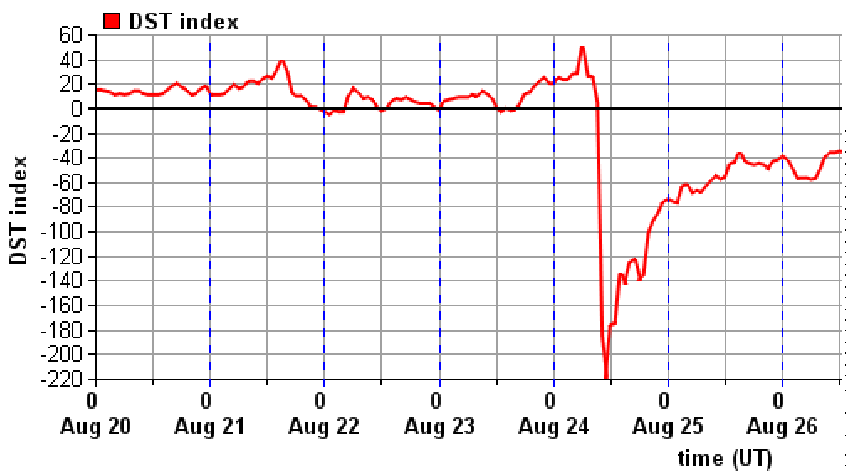

DST index
DST index
Aug 20
Aug 21
Aug 22
Aug 23
Aug 24
Aug 25
Aug 26
time (UT)


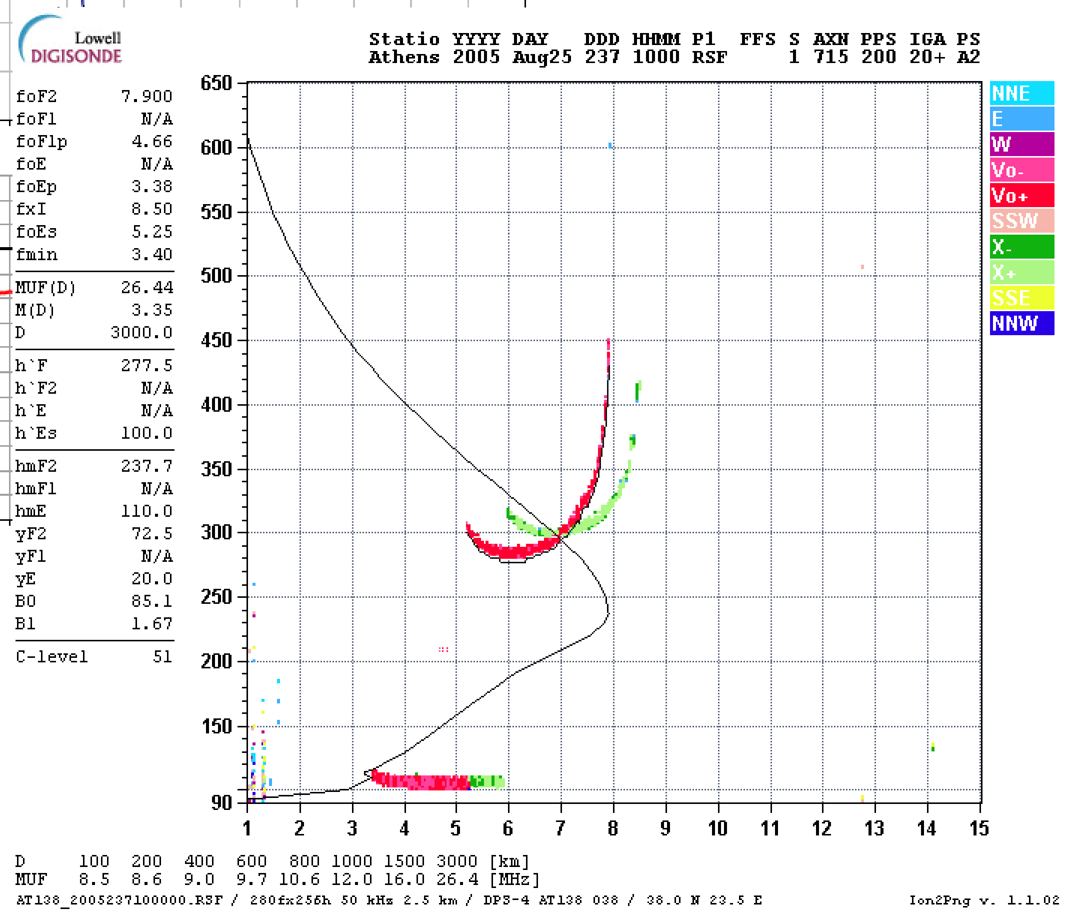

Lowell DIGISONDE
Statio YYYY DAY DDD HHMM P1 FFS S AXN PPS IGA PS
Athens 2005 Aug25 237 1000 RSF 1 715 200 20+ A2
foF2 7.900
foF1 N/A
foF1p 4.66
foE N/A
foEp 3.38
fxI 8.50
foEs 5.25
fmin 3.40
MUF(D) 26.44
M(D) 3.35
D 3000.0
h`F 277.5
h`F2 N/A
h`E N/A
h`Es 100.0
hmF2 237.7
hmF1 N/A
hmE 110.0
yF2 72.5
yF1 N/A
yE 20.0
B0 85.1
B1 1.67
C-level 51
NNE
E
W
Vo-
Vo+
SSW
X-
X+
SSE
NNW
D 100 200 400 600 800 1000 1500 3000 [km]
MUF 8.5 8.6 9.0 9.7 10.6 12.0 16.0 26.4 [MHz]
AT138_2005237100000.RSF / 280fx256h 50 kHz 2.5 km / DPS-4 AT138 038 / 38.0 N 23.5 E
Ion2Png v. 1.1.02

# The ITEC parameter

The topside profiler: a-Chapman function, assuming constant topside scale height $H_T$ (Huang and Reinisch, Radio Science, 2001)

$$N(h) = N_m \exp[\tfrac{1}{2}(1 - z - e^{-z})]; \qquad z = \frac{h - hmF2}{H_T}$$

$H_T = H_m$ at the F2 layer peak.

$H_m$ can be calculated from the known bottomside function N(h)

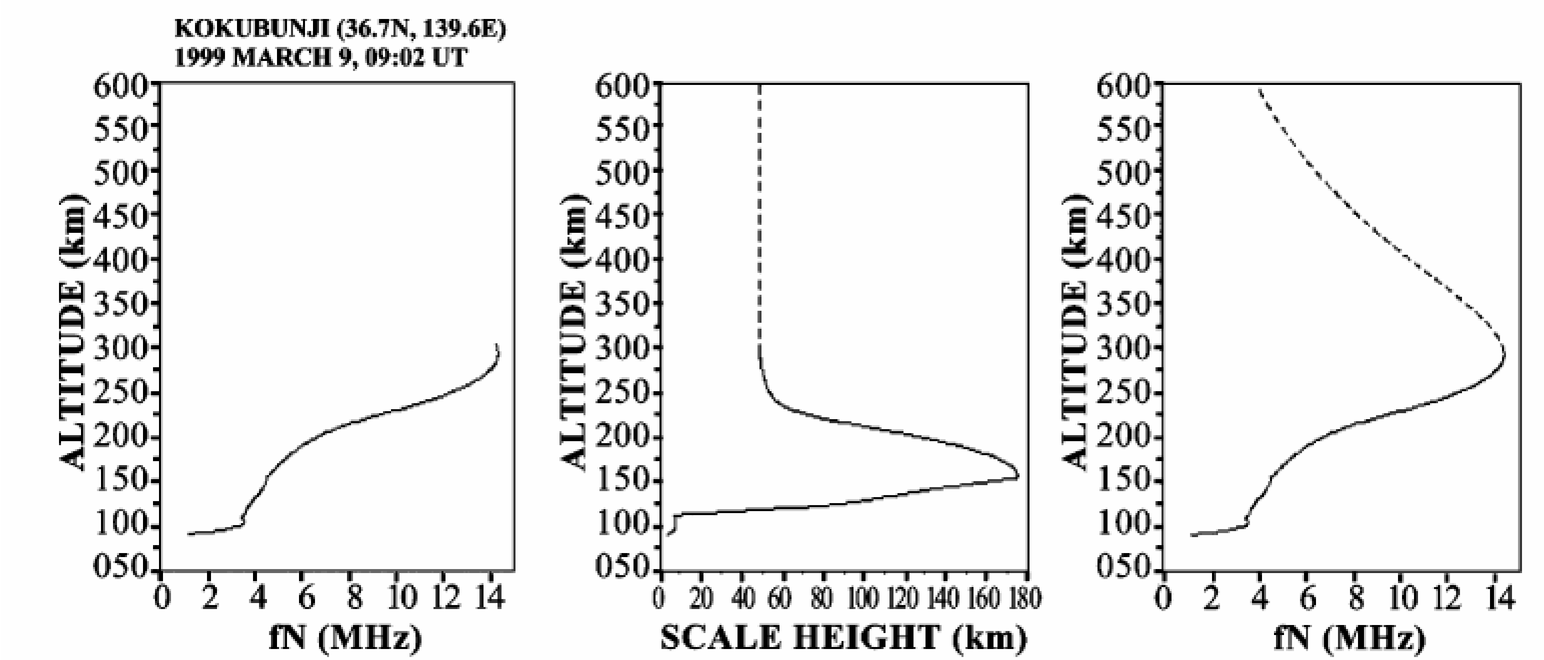


*(Reinisch et al., ASR 2004)*

# ITEC quantitative validation

**Data source:** 4,000 ISR profiles from Malvern in UK (1968-1972) – up to 700 km

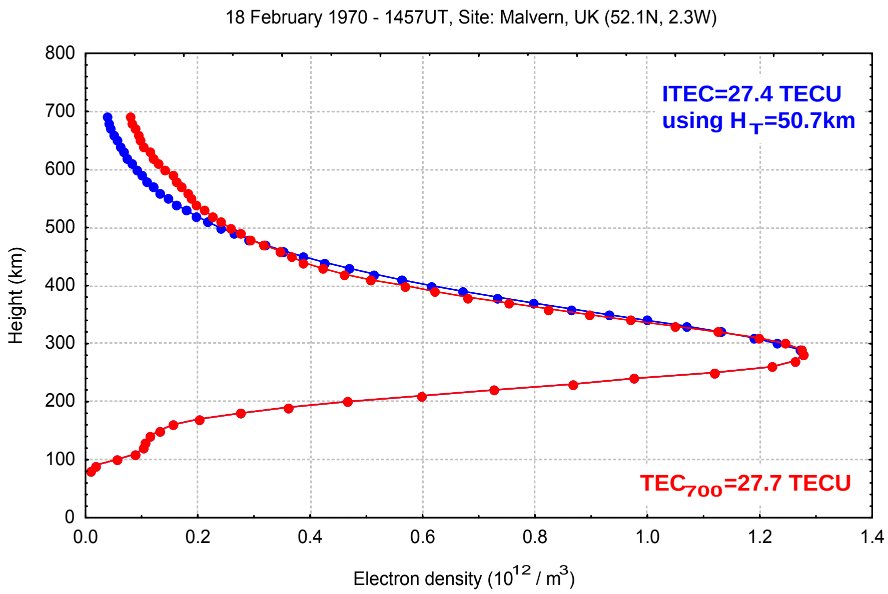


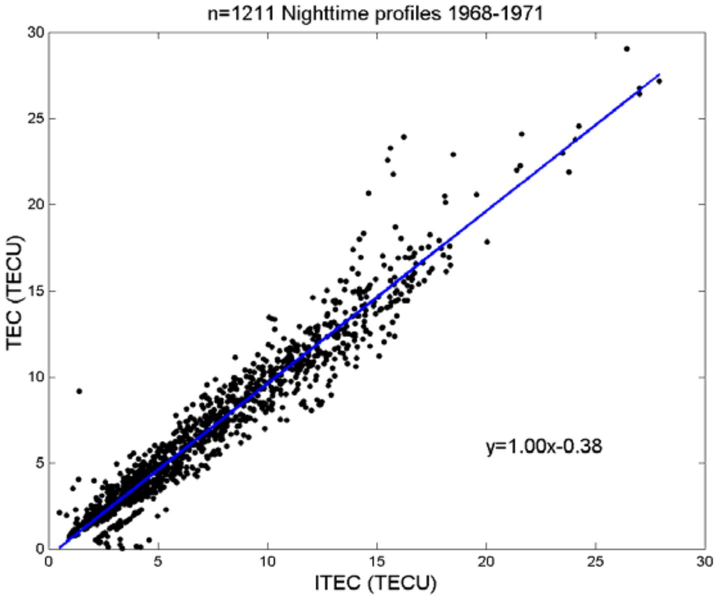


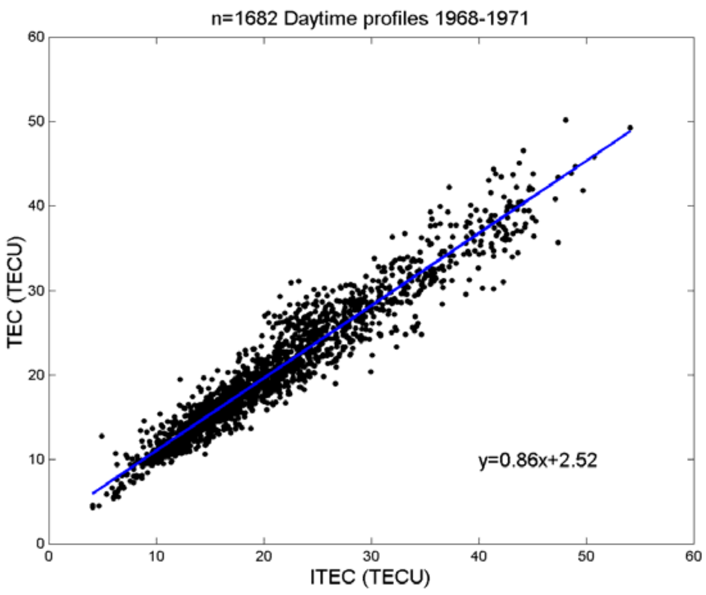


*(Belehaki and Kersley, Radio Science, 2006)*

# Ionospheric Drift Measurements

Three main processes are creating ionospheric drifts.

a) Gradient drift $$u_{gd} = \frac{\varepsilon_{\perp} + 2\varepsilon_{\parallel}}{qB^3}(\overline{B} \times \nabla_{\perp}|B|)$$

b) Electric field drift $$u_{ed} = \frac{1}{B^2}(\overline{E} \times \overline{B})$$

c) Drift due to gravity $$u_{ed} = \frac{q}{mB^2}(\overline{g} \times \overline{B})$$

Two more mechanisms cause movement of ionospheric plasma:
a) neutral winds
b) traveling ionospheric disturbances (TID’s)

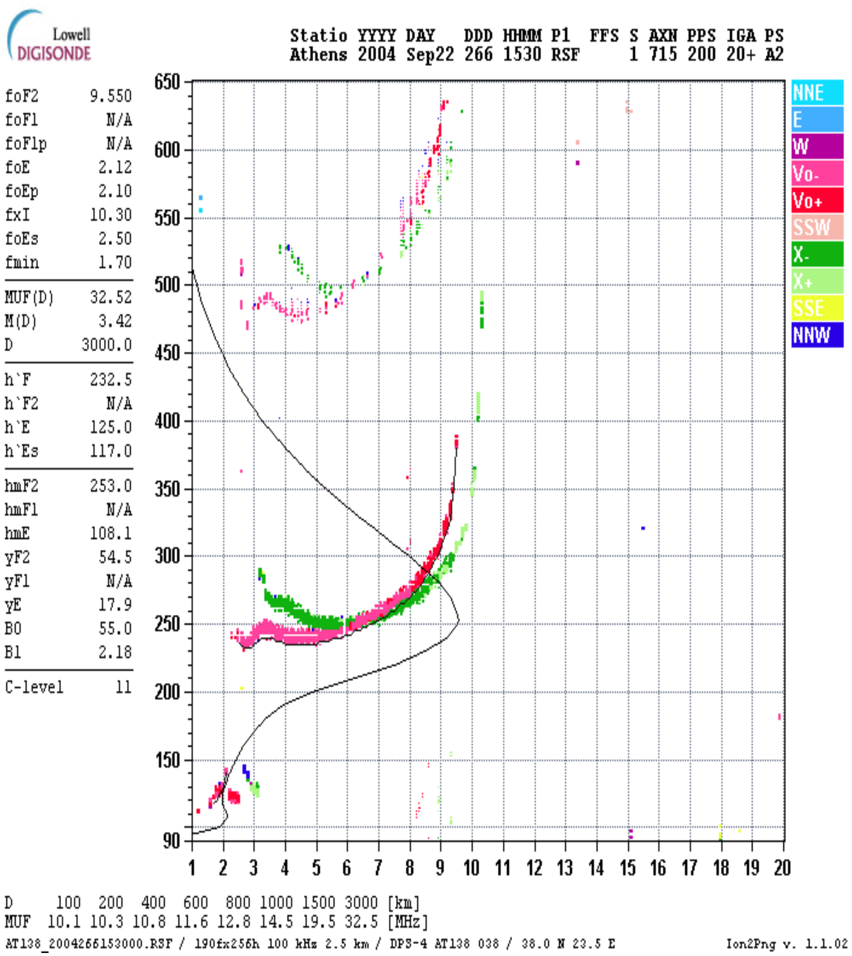
Lowell
DIGISONDE
Statio YYYY DAY DDD HHMM P1 FFS S AXN PPS IGA PS
Athens 2004 Sep22 266 1530 RSF 1 715 200 20+ A2
foF2 9.550
foF1 N/A
foF1p N/A
foE 2.12
foEp 2.10
fxI 10.30
foEs 2.50
fmin 1.70
MUF(D) 32.52
M(D) 3.42
D 3000.0
h`F 232.5
h`F2 N/A
h`E 125.0
h`Es 117.0
hmF2 253.0
hmF1 N/A
hmE 108.1
yF2 54.5
yF1 N/A
yE 17.9
B0 55.0
B1 2.18
C-level 11
NNE
E
W
Vo-
Vo+
SSW
X-
X+
SSE
NNW
D 100 200 400 600 800 1000 1500 3000 [km]
MUF 10.1 10.3 10.8 11.6 12.8 14.5 19.5 32.5 [MHz]
AT138_2004266153000.RSF / 190fx256h 100 kHz 2.5 km / DPS-4 AT138 038 / 38.0 N 23.5 E
Ion2Png v. 1.1.02

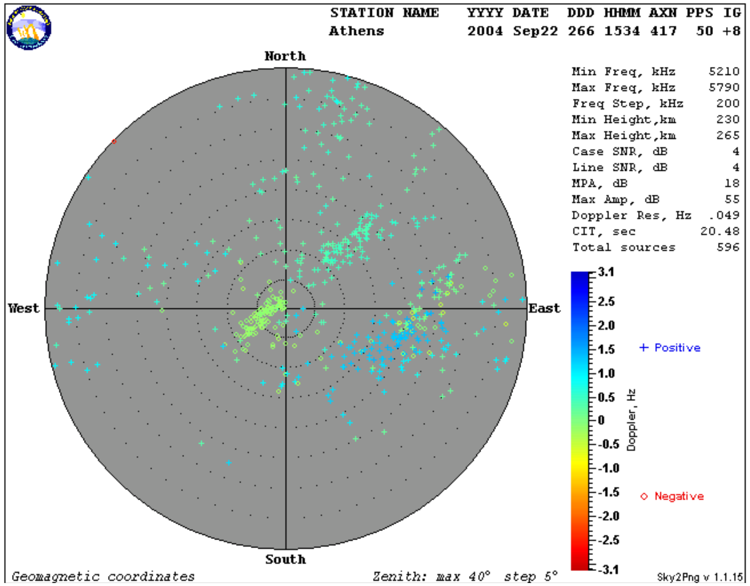
STATION NAME YYYY DATE DDD HHMM AXN PPS IG
Athens 2004 Sep22 266 1534 417 50 +8
North
West
East
South
Min Freq, kHz 5210
Max Freq, kHz 5790
Freq Step, kHz 200
Min Height,km 230
Max Height,km 265
Case SNR, dB 4
Line SNR, dB 4
MPA, dB 18
Max Amp, dB 55
Doppler Res, Hz .049
CIT, sec 20.48
Total sources 596
+ Positive
◇ Negative
Doppler, Hz
Geomagnetic coordinates
Zenith: max 40° step 5°
Sky2Png v 1.1.15

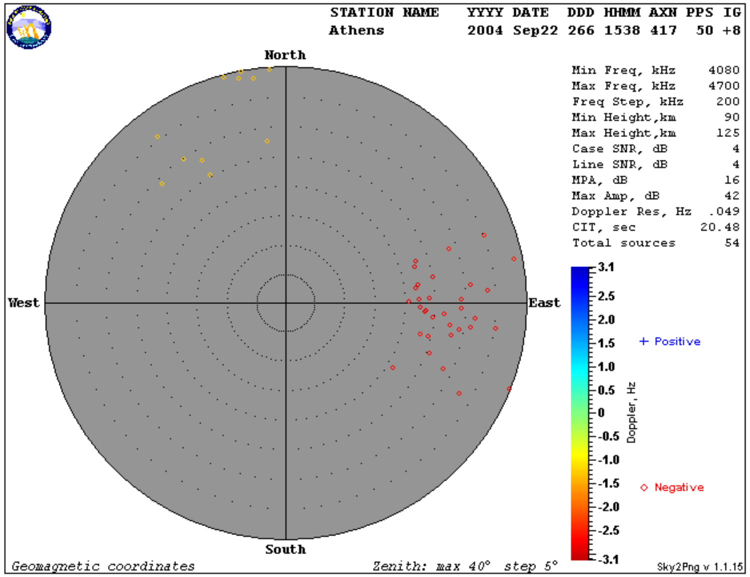
STATION NAME YYYY DATE DDD HHMM AXN PPS IG
Athens 2004 Sep22 266 1538 417 50 +8
North
West
East
South
Min Freq, kHz 4080
Max Freq, kHz 4700
Freq Step, kHz 200
Min Height,km 90
Max Height,km 125
Case SNR, dB 4
Line SNR, dB 4
MPA, dB 16
Max Amp, dB 42
Doppler Res, Hz .049
CIT, sec 20.48
Total sources 54
+ Positive
◇ Negative
Doppler, Hz
Geomagnetic coordinates
Zenith: max 40° step 5°
Sky2Png v 1.1.15

# Independent monitoring of E and F region drift motions (Belehaki et al., 2006)

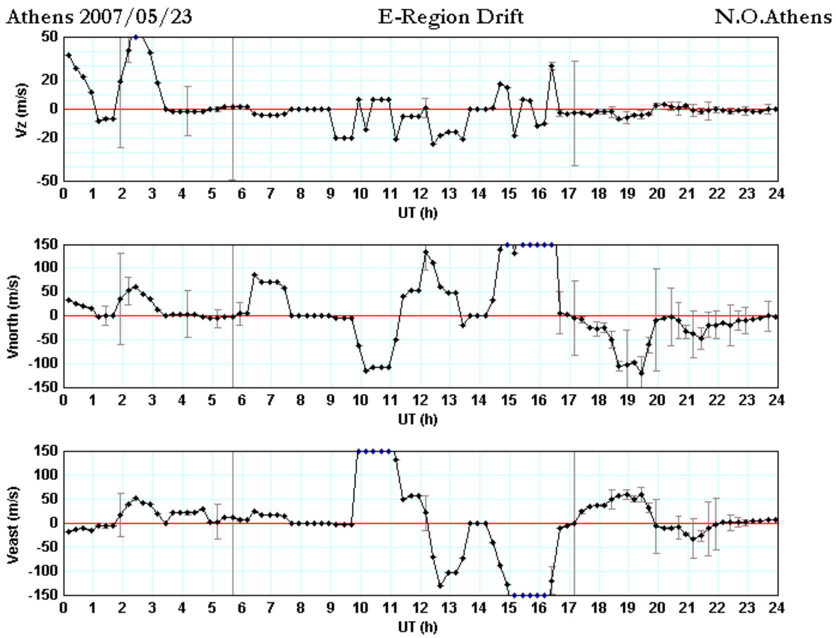


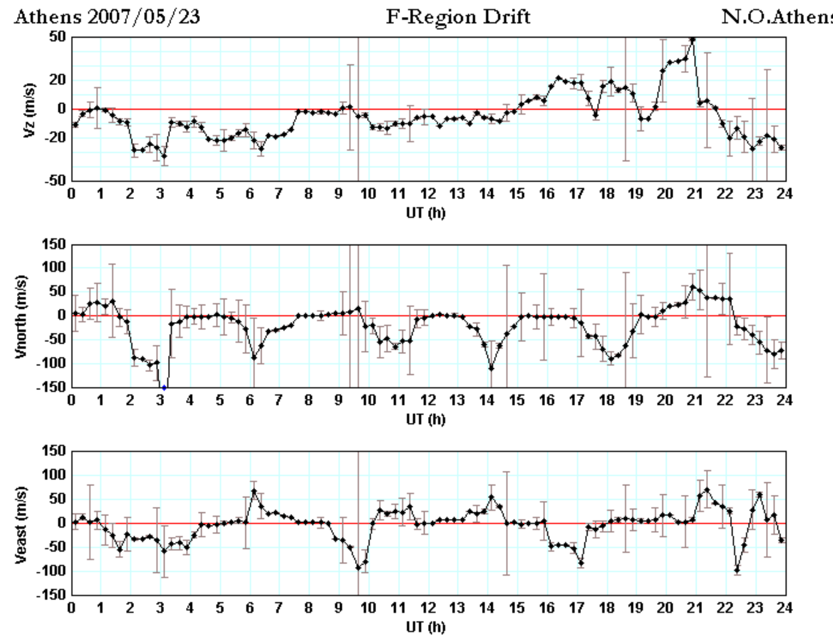


**http://www.iono.noa.gr**

# Ionospheric models rely on the availability of real-time data from networks of stations over large areas

- Lowell DDIB (post processing of ionograms)
- DIAS (ionospheric specification and prediction in Europe)
- IPS (ionospheric specification and prediction in Australia)
- SPIDR (database of historical ionospheric data and visualization tools)

# Lowell Network of Digisondes (UMAS Lowell)

# DIAS system (National Observatory of Athens)

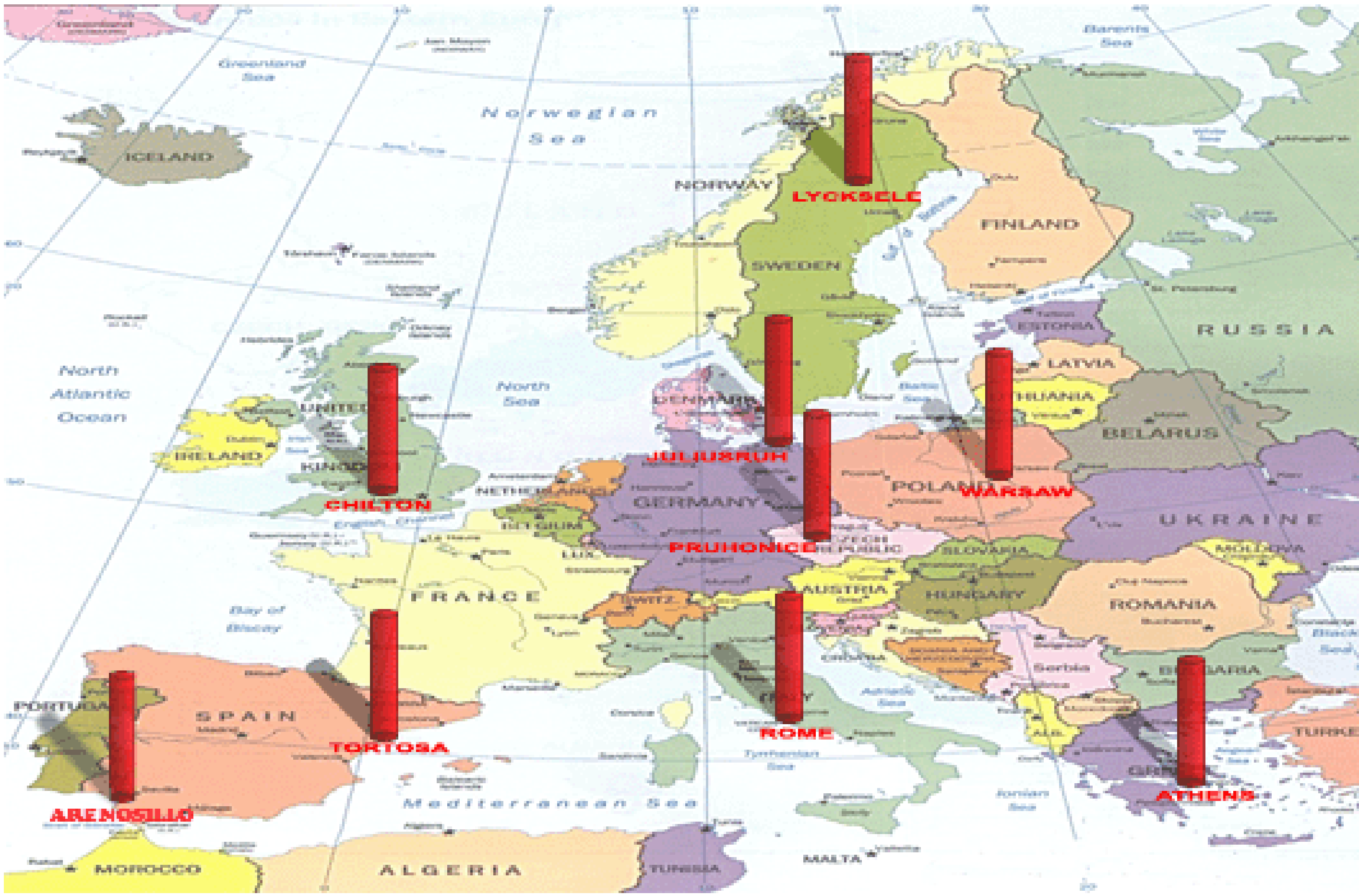


**http://dias.space.noa.gr**

# DIAS products

## 1. Ionospheric specification

• Ionograms with the results of the automatic scaling
• Ionospheric scaled parameters (f-plots)
• Electron Density Ne(h) profiles over each DIAS station
• Maps of foF2, M(3000)F2, MUF and Ne over Europe
• Daily plots of the Effective Sunspot Number
• Point to point calculation of the *MUF* for user-defined coordinates

## 2. Ionospheric Prediction, Forecast and Warning

• Long term ionospheric predictions for the next 3 months (maps of foF2, M(3000)F2 and MUF)
• Short-term ionospheric forecasting 24 hours ahead (maps of *foF2,* plots of the forecasted *foF2* over each DIAS station)
• Ionospheric Activity Index (alerts and warnings)

# SEE 2007

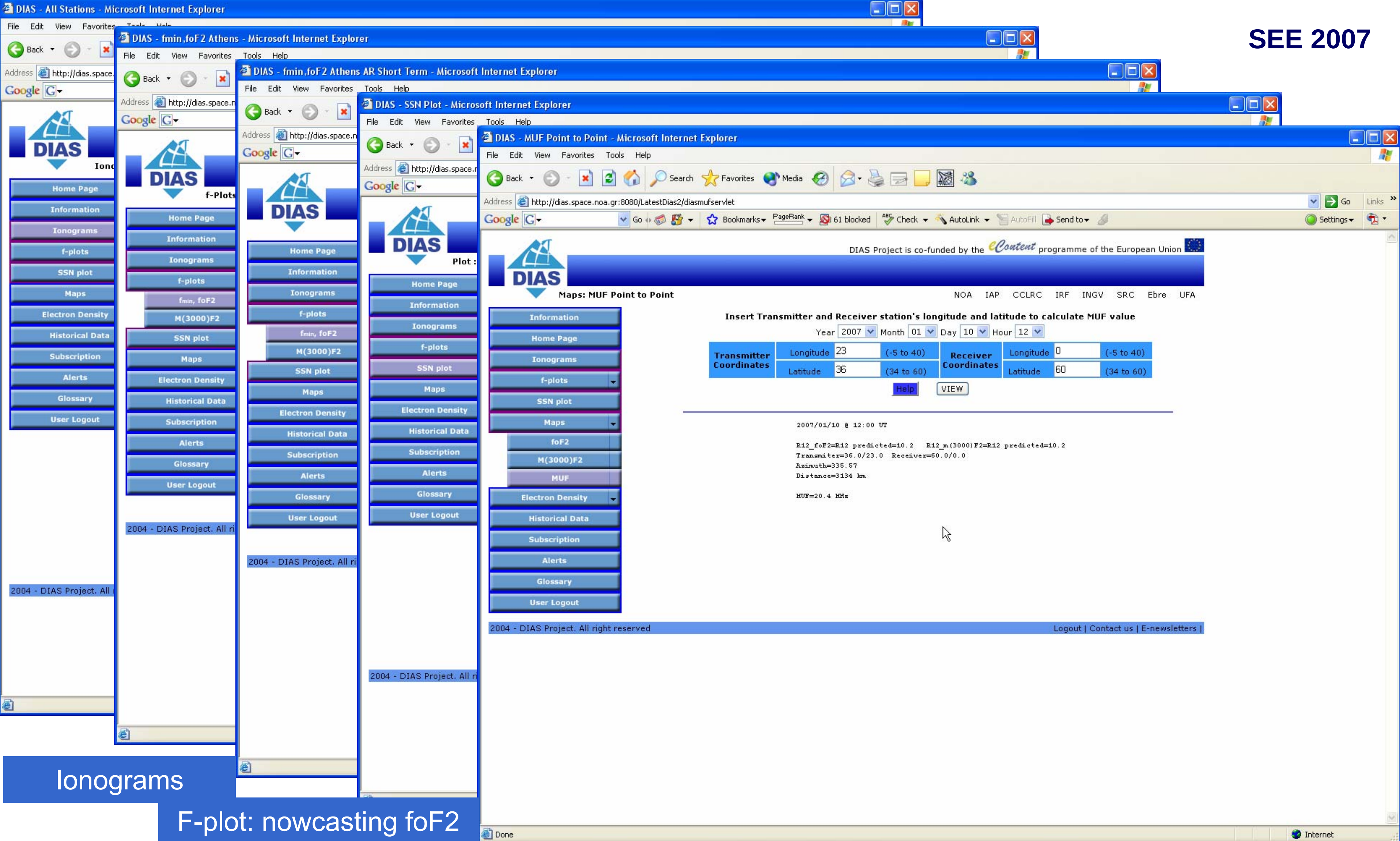


Ionograms

F-plot: nowcasting foF2

F-plot: forecasting foF2

SSN daily plot

MUF Point to Point

# SEE 2007

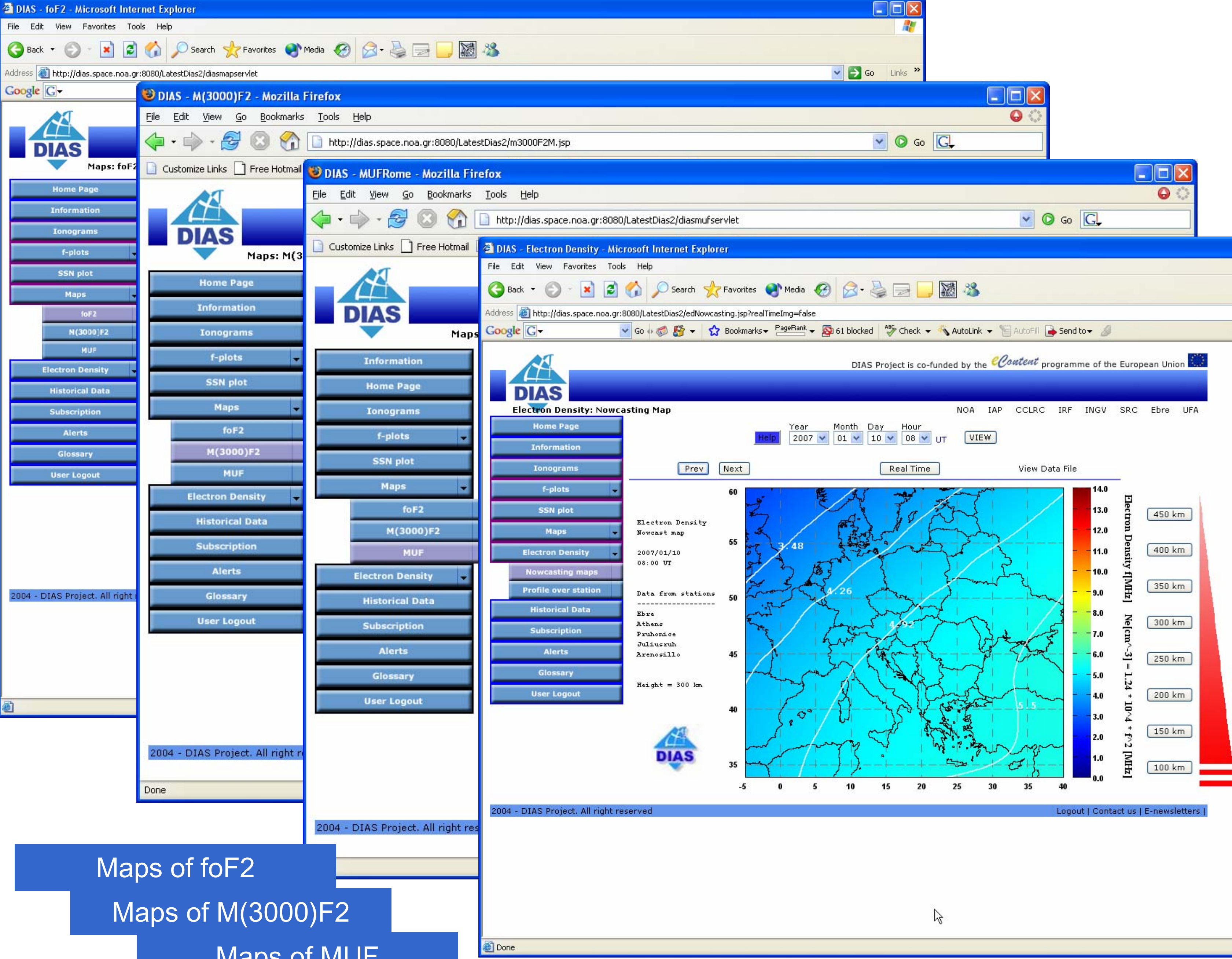


Maps of foF2

Maps of M(3000)F2

Maps of MUF

Maps of Ne

# Ionospheric Storms

- Changes in the bottom ionosphere (observed by ground ionosondes)
- Changes in the topside ionosphere (studied by model extrapolation of the Ne(h) profile and observed by space-based sounders)
- Changes in the plasmasphere (studies by plasmaspheric models supported by radio plasmaspheric imagers)

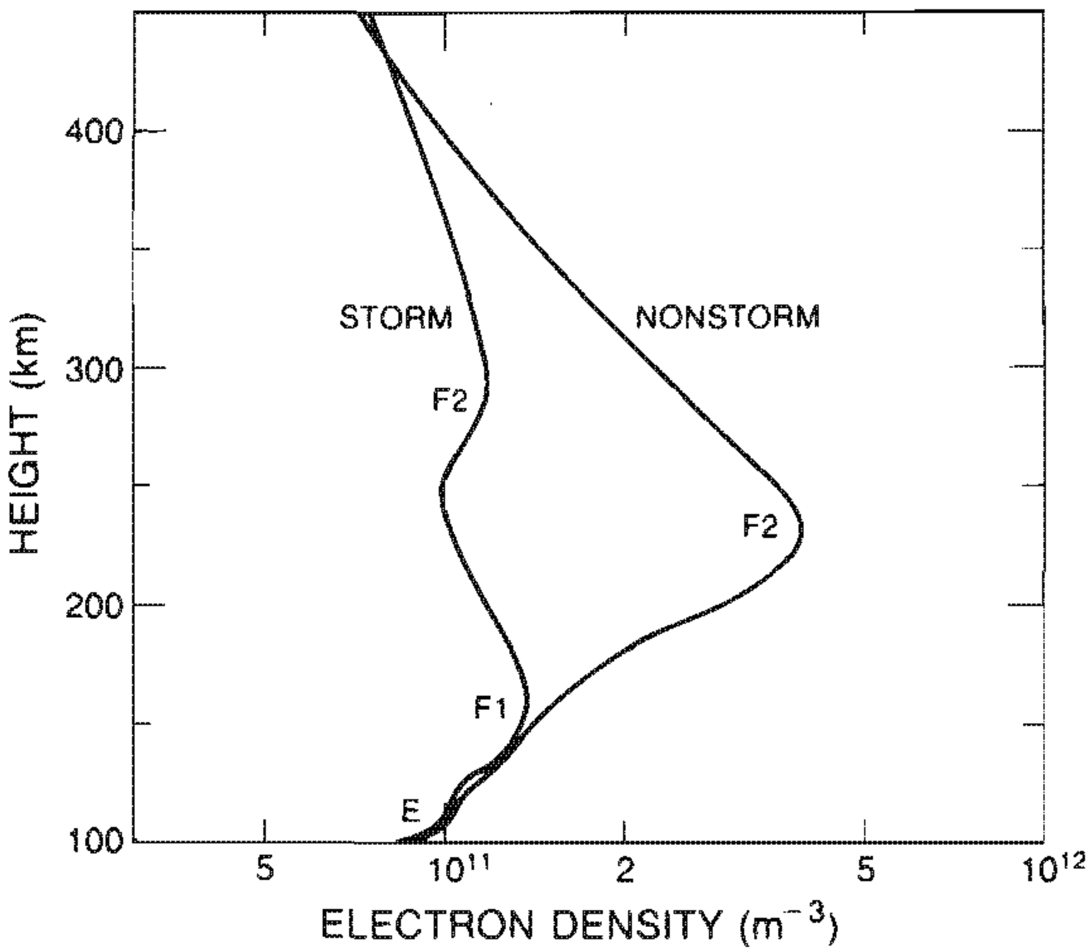

HEIGHT (km)
400
300
200
100
5
$10^{11}$
2
5
$10^{12}$
ELECTRON DENSITY ($m^{-3}$)
STORM
NONSTORM
F2
F2
F1
E

# I-T storms

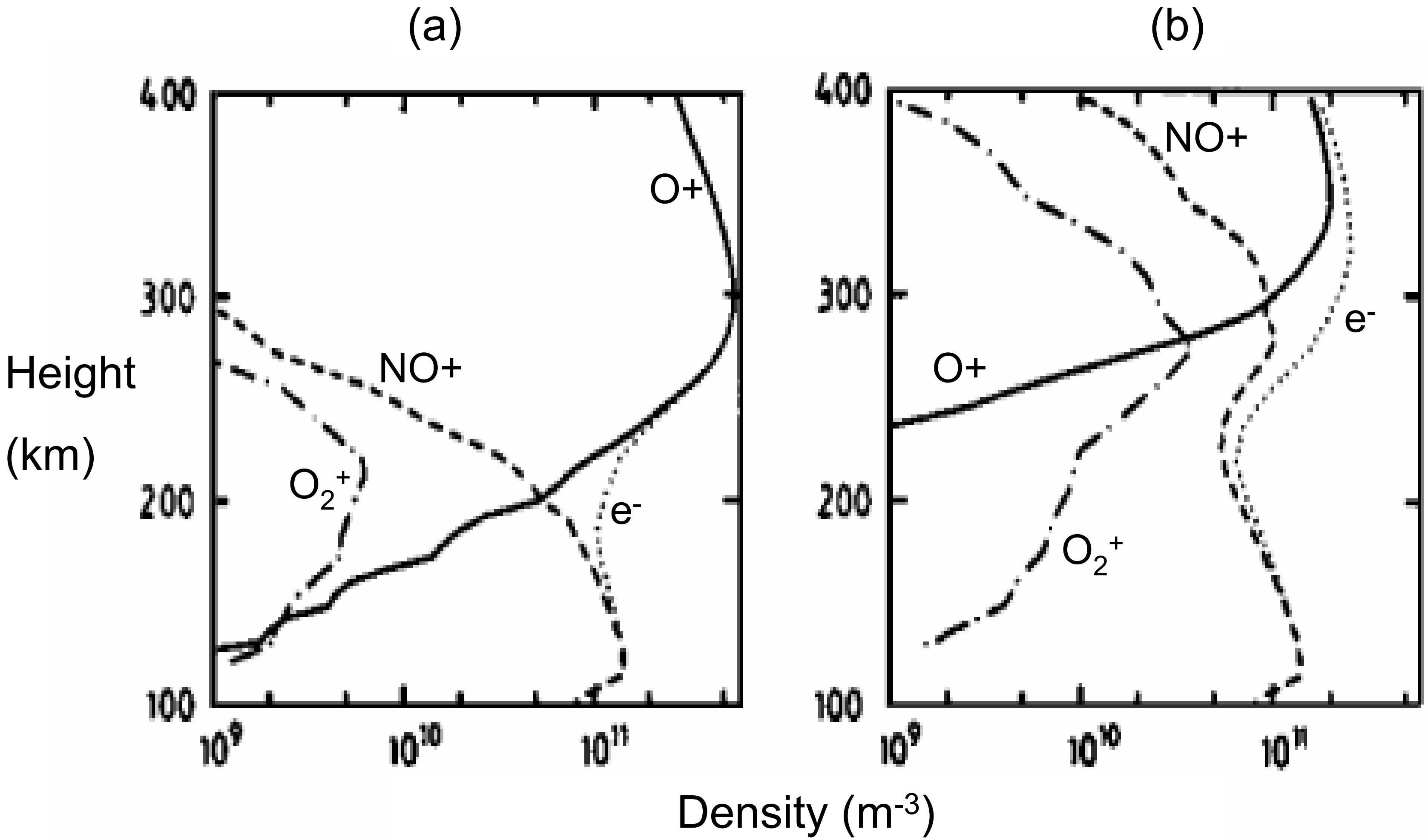


Height profiles of density for ions and electrons (dotted line) for (a) quiet conditions and (b) disturbed conditions at high latitudes (Millward et al., 1993).

# Drivers of the I-T system during geomagnetic storms

1. Enhanced high-energy particle precipitation **[important at altitudes lower than F2 layer]**
2. Enhanced ionospheric electric currents and resulting Joule heating **[global importance]**
3. Enhanced electric fields predominantly of magnetospheric origin **[importance at higher latitude and penetrate to equatorial region]**
4. At high latitudes frictional heating, primarily induced by enhanced magnetospheric convection **[importance at high latitudes]**

The enhanced Joule heating is globally the most important factor producing the thermospheric storm.

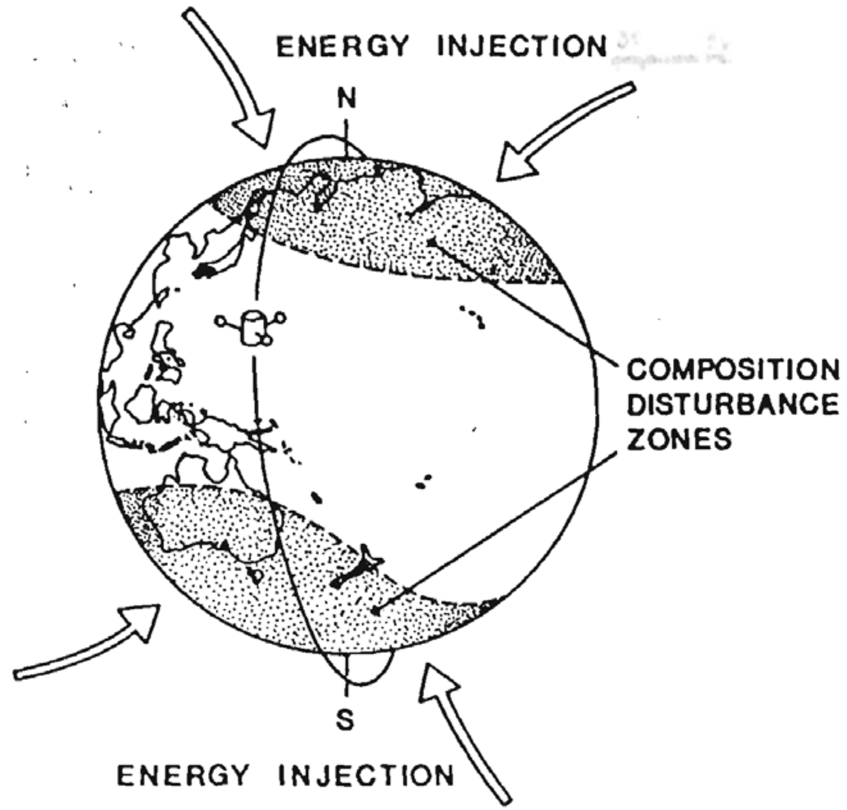


The resulting slow ionization loss by recombination, i.e. neutral atmosphere processes including dynamics have sufficient time available to affect the ionized component substantially (I-T coupling).

(from Prölss, Handbook of Atmospheric Electrodynamics, 1995)

# Ionospheric storms: local-time dependent scenario

## Prölss phenomenological model:

The station located in the afternoon sector during the expansion phase does not experience the negative phase of the ionospheric storm.

The station located in the early morning sector observes well the ionospheric storm. During strong and long storms, the negative phase reaches lower latitudes, lasts longer and may “occupy” the whole midlatitude area.

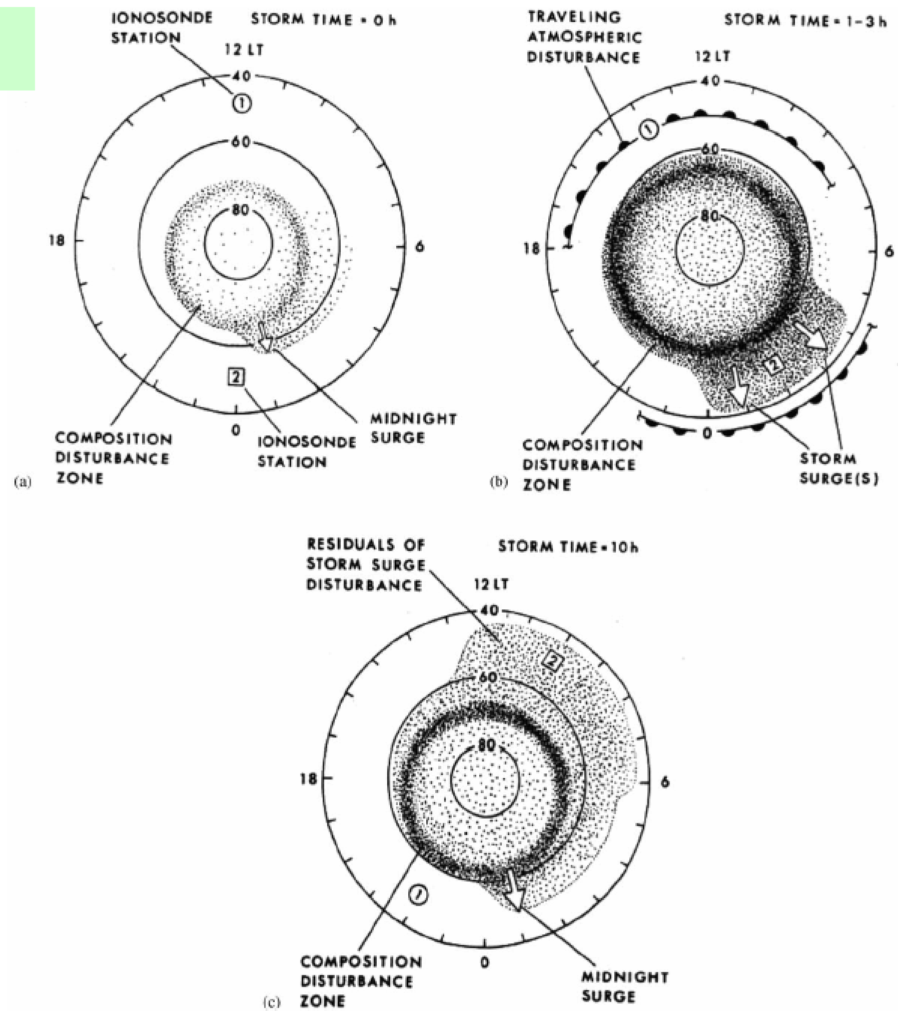


*After Prölss, 1996*

# Prölss phenomenological model: positive and negative storm effects

Negative storm effects: The negative phase is predominantly an ionospheric response to the thermospheric disturbance, to a change of composition due to heating of the thermosphere.

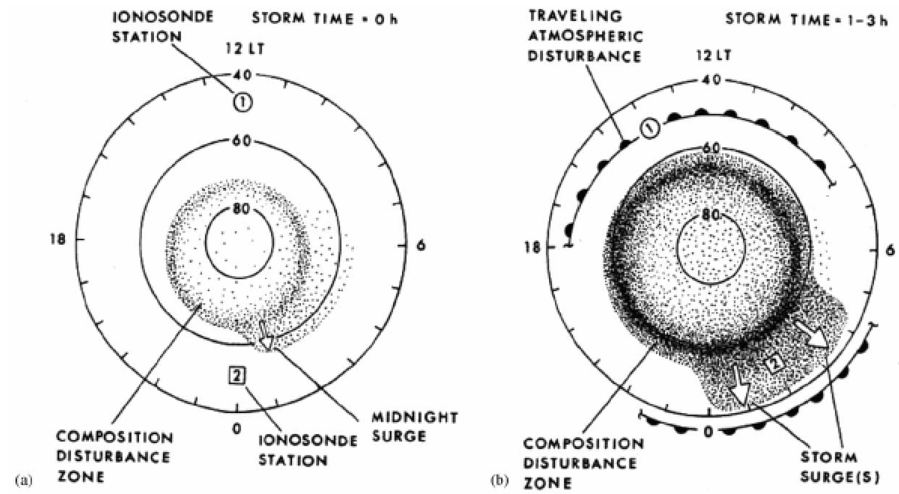


Positive storm effects: During the day TADs propagate from auroral zone to lower latitudes. This disturbance propagates with storm-induced meridional wind pushing ionization upward along geomagnetic field lines. This results in an increase of hmaxF2 and an increase of NmaxF2 (and=or foF2) due to lower electron loss rate at higher altitudes. At night lack of ionization production diminishes their formation.

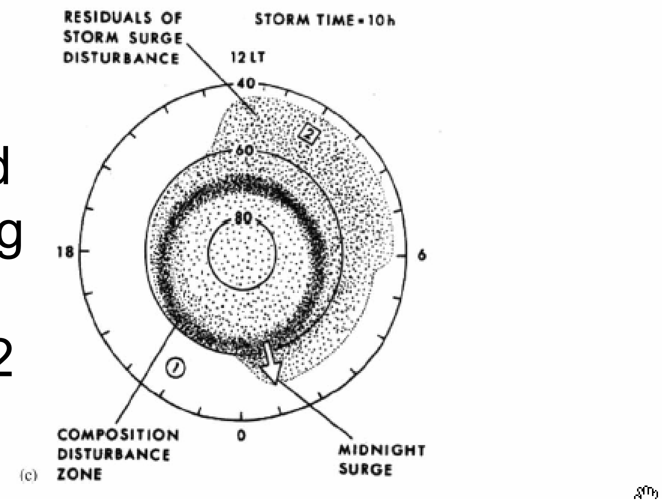

# Capturing night-time positive storm effects

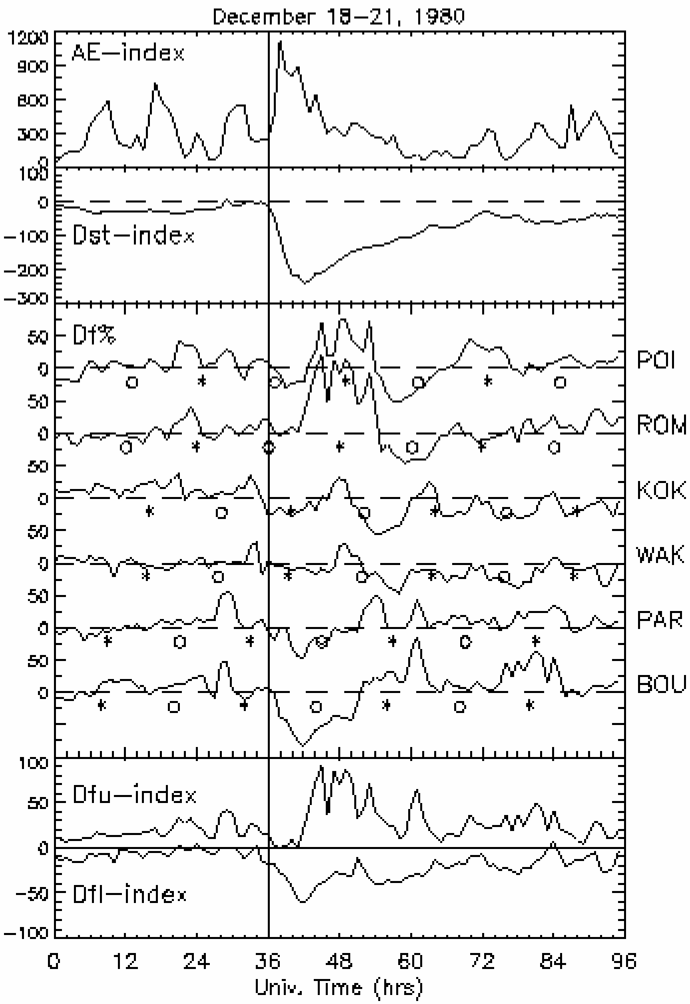


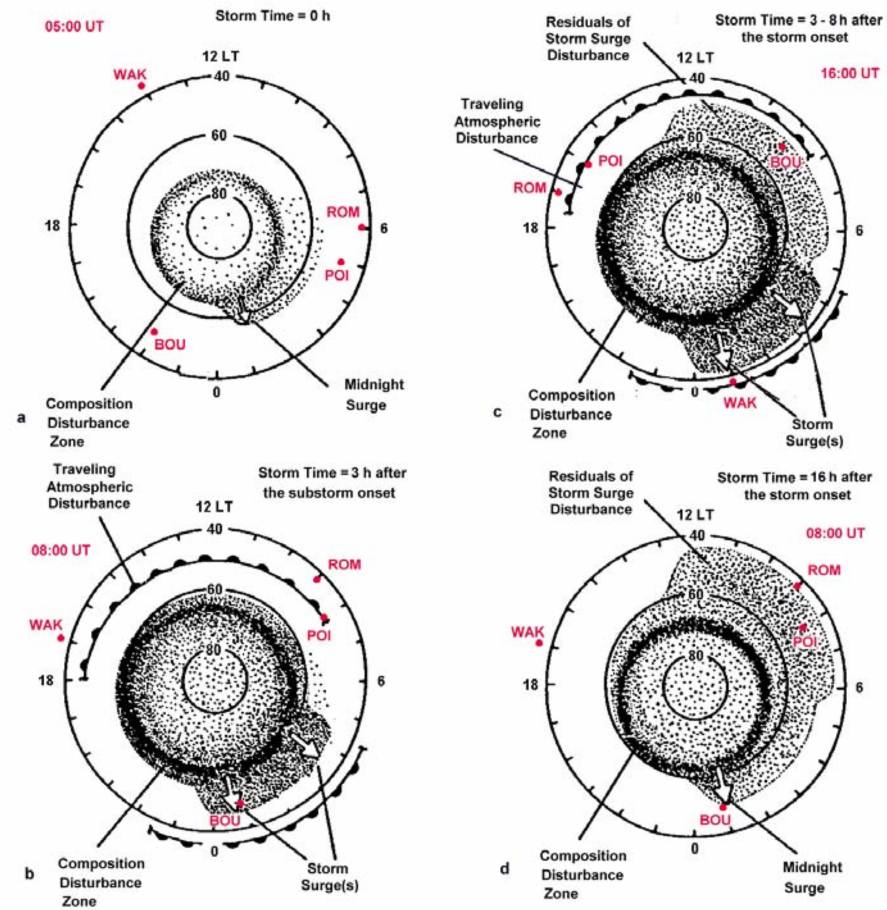


*After Tsagouri et al., GRL 2000*

A possible thus explanation for their generation may be consistent with the point of Fuller-Rowell et al. (1994) suggesting that if a positive phase is driven by winds before dusk it will rotate into the night side.

# Ionospheric forecast models

- autocorrelation methods (based on the past history)
- multi-regression methods (using geomagnetic indices as drivers)
- neural networks (based on the past history and / or using geomagnetic parameters as drivers.

# Short term ionospheric forecast models implemented on DIAS system

- GCAM: Linear Regressive Model

"Geomagnetically Correlated Autoregression Model" by Kutiev, Muhtarov and Cander, Journal of Inverse Problems, 2002.

- TSAR: Time Series Autoregressive model

by Koutroumbas, Tsagouri, Belehaki, Annales Geophysicae, 2007 (submitted)

# GCAM model

Predicted variable: $\Phi = (fof2 - fof2median)/fof2median$

Prediction time is at k=0 and k=1,..,n past values are used

$$\Phi_0 = \overline{\Phi} + \boxed{\sum_{k=1}^{n} \beta_k (\Phi_k - \overline{\Phi})} + \boxed{\sum_{k=0}^{n} \gamma_k (G_k - \overline{G})}$$

Part depending on the past n values of Φ

Part depending on the past n values and the value for the time of prediction of the magnetic activity index G .

When this part is ommitted the model depends only on autocorrelation

*$\overline{\Phi}$, $\overline{G}$ : Mean values of $\Phi$, G typically for the past 25 days*

# GCAM prediction performance

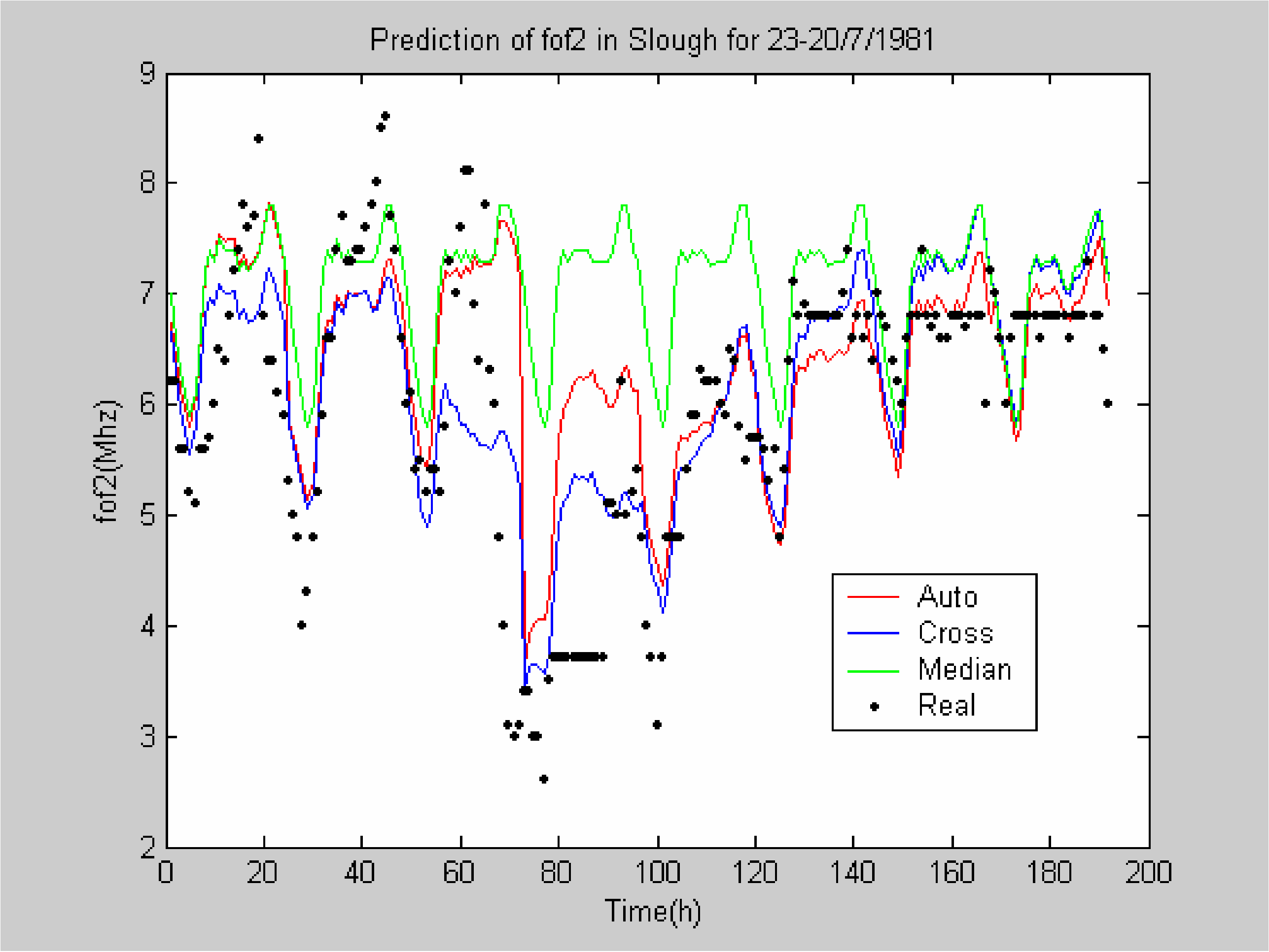

# TSAR model: foF2 prediction using AR models

The *foF2* values are taken every 15mins.

**Aim**: Estimation of *foF2* after:
15mins (*s*=1), 1hour (*s*=4), 2hours (*s*=8), …, 24hours (*s*=96)

25 AR models are employed:
AR0 (15mins), AR1 (1hour), AR2 (2hours),…, AR24 (24hours)

**Estimation of ARs**:
Each of the 25 AR models is re-esimated at the beginning of each month as follows:
- Define *X1* as the time series segment of the 1st half of the previous month (training set)
- Define *X2* as the time series segment of the 2nd half of the previous month (test set)
- Apply *BMDM (Best Model Determination method).*

**Estimation of the foF2 values**:After its estimation, each ARi is applied every time a new observation becomes available.

# Linear or non-linear ionospheric response?

<u>TSAR</u> performance is compared with predictions obtained using a similar method that, instead of AR models, it uses feedforward neural networks with a single hidden layer (<u>TSNN</u>).

# TSAR-TSNN comparison (Storm conditions)

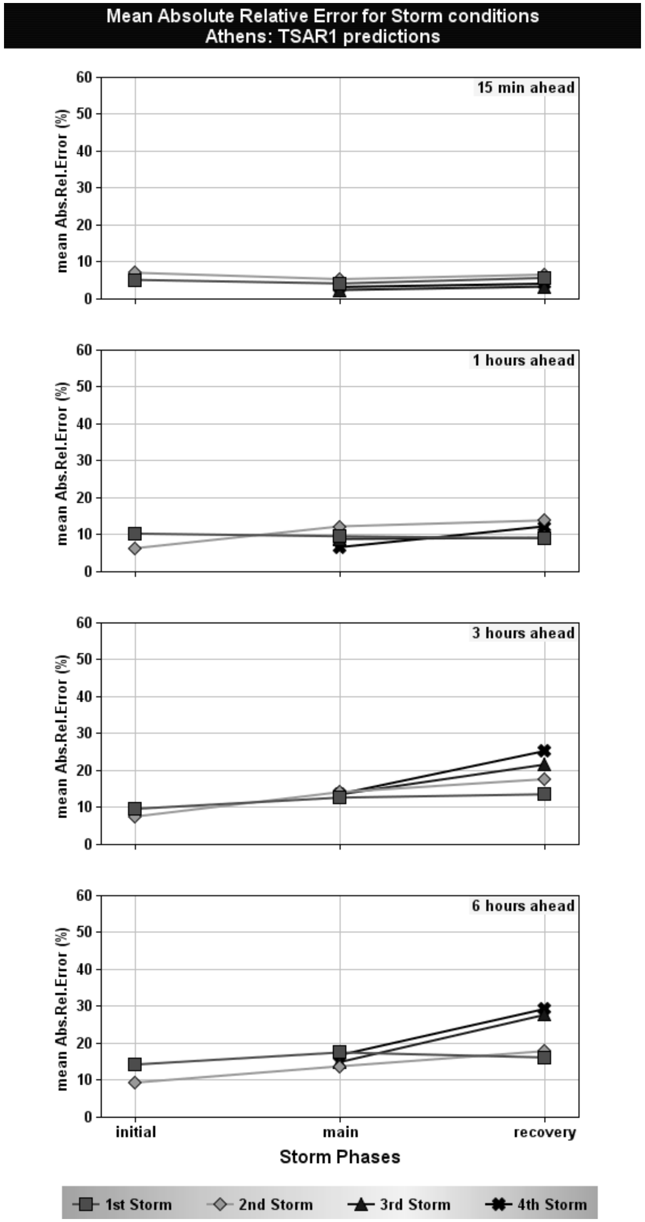


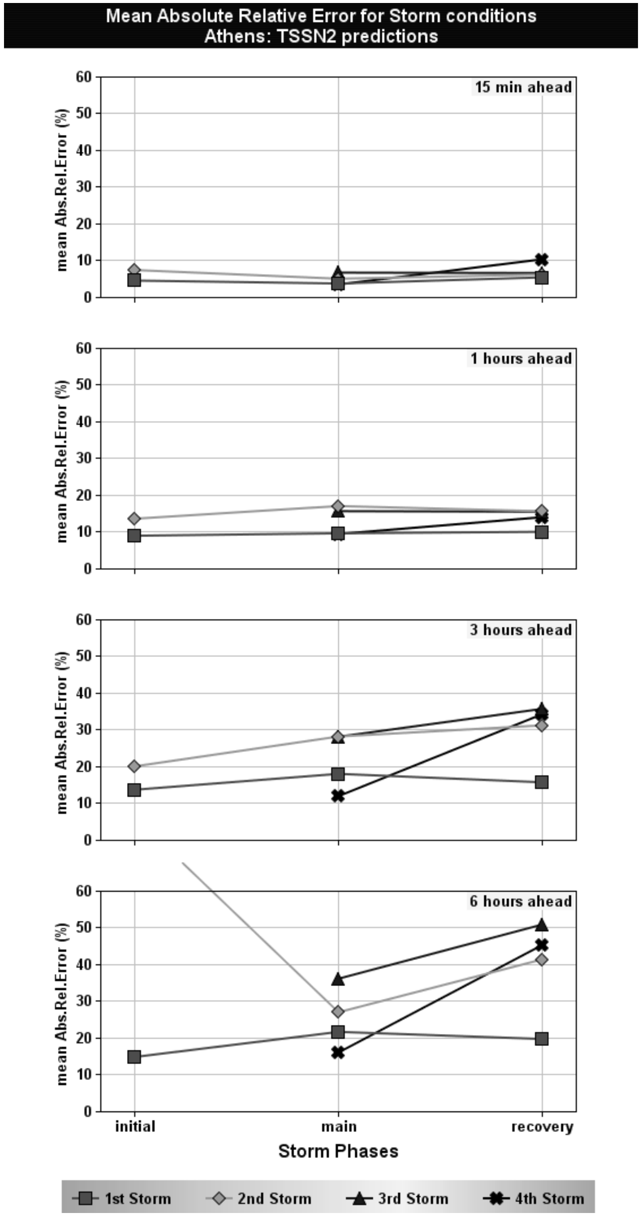

# GCAM-TSAR comparison (Storm conditions)

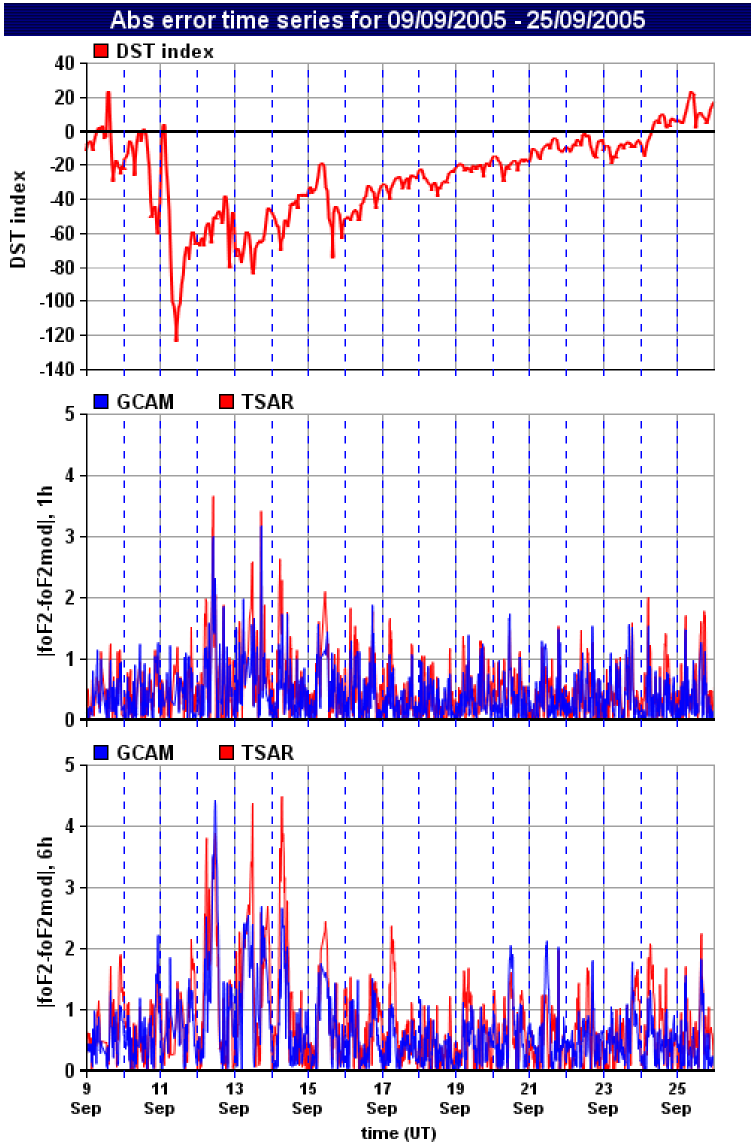


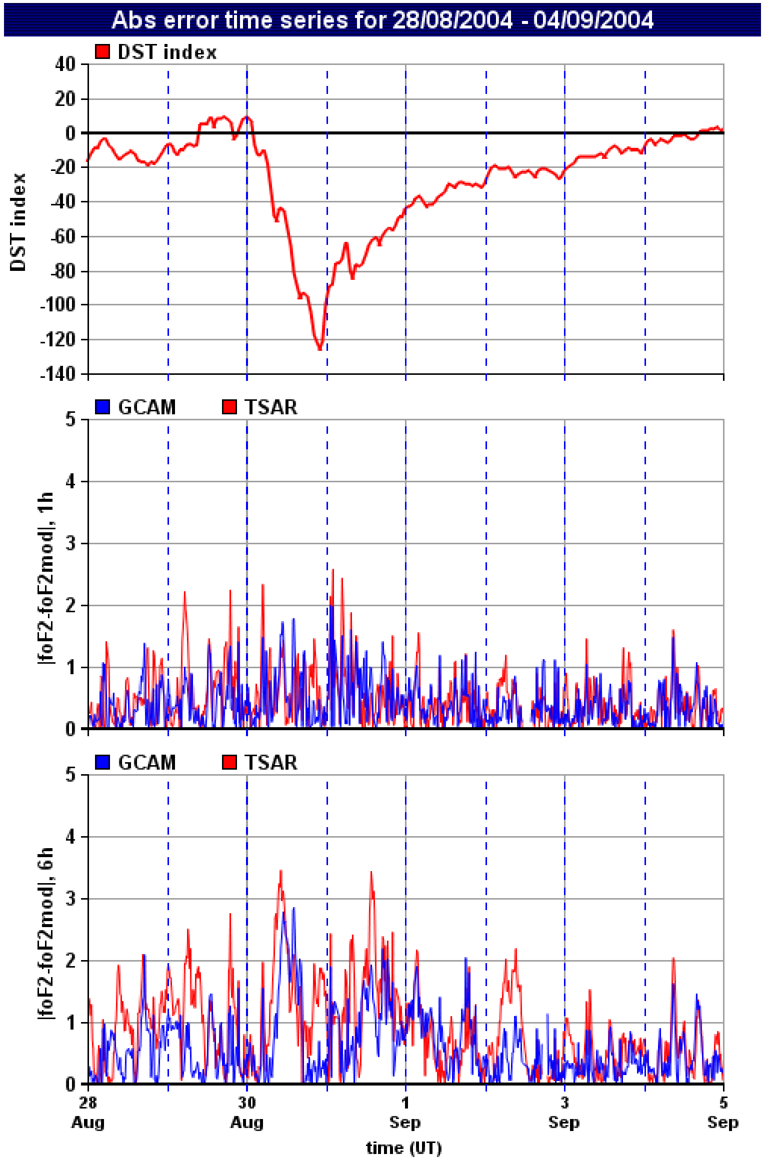

# GCAM-TSAR comparison (Storm conditions)

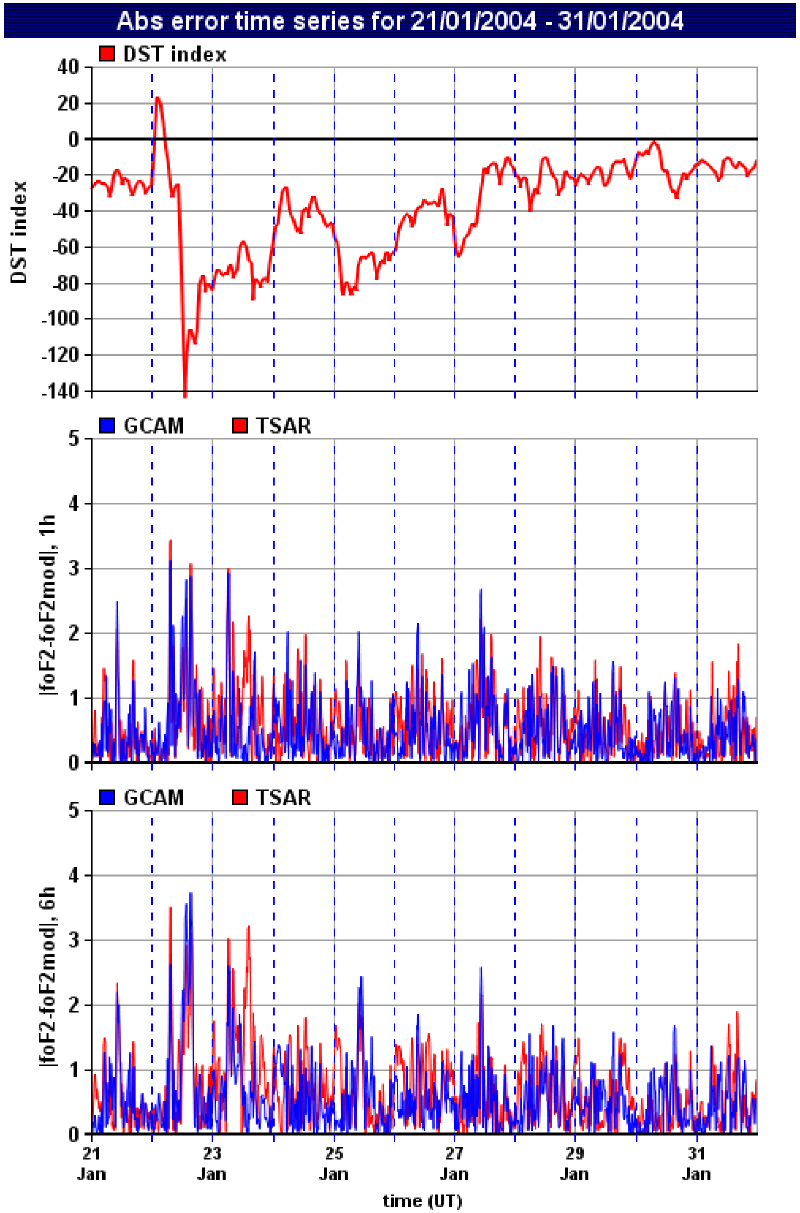


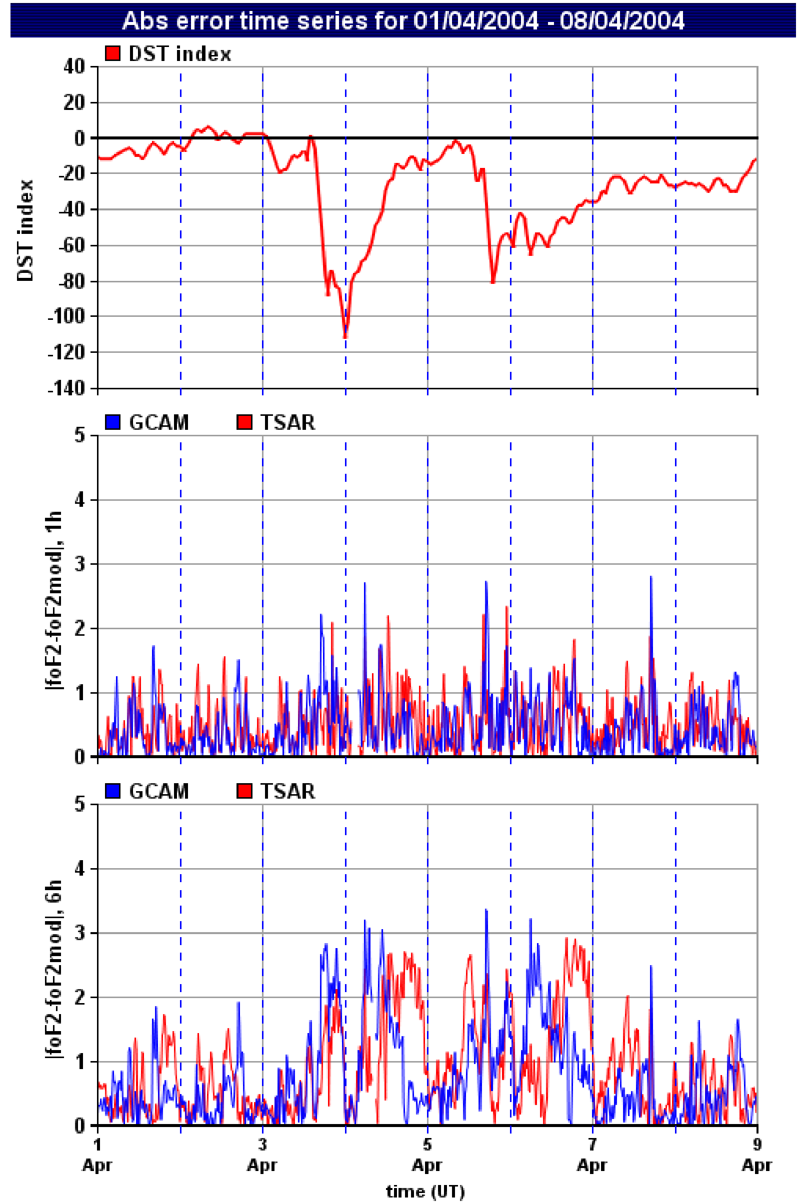

# GCAM-TSAR comparison (Quiet conditions)

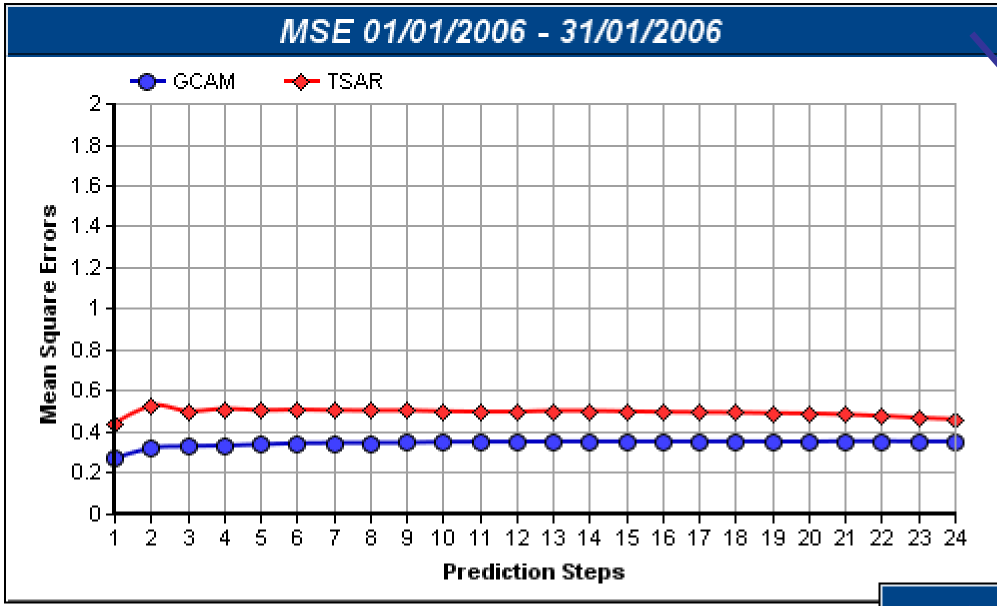


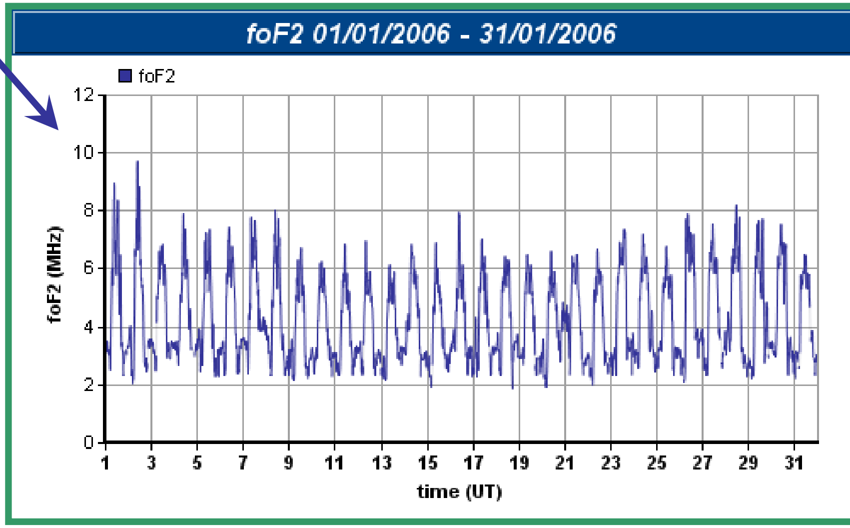


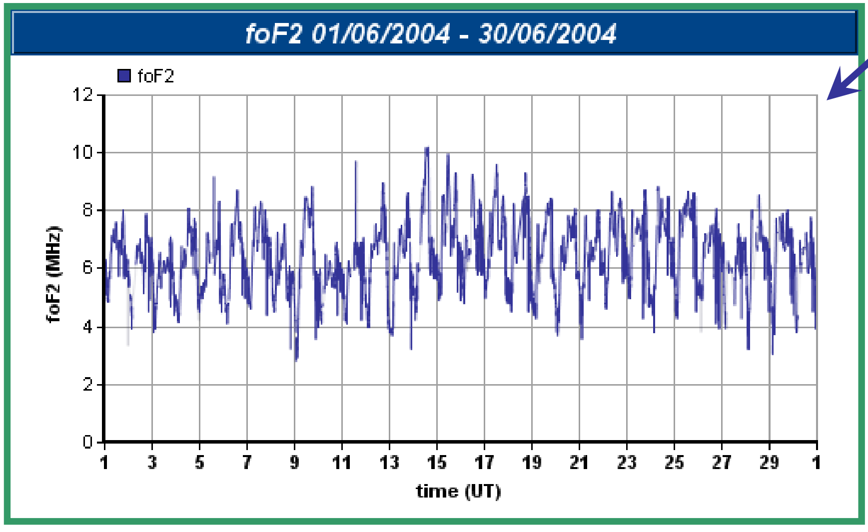


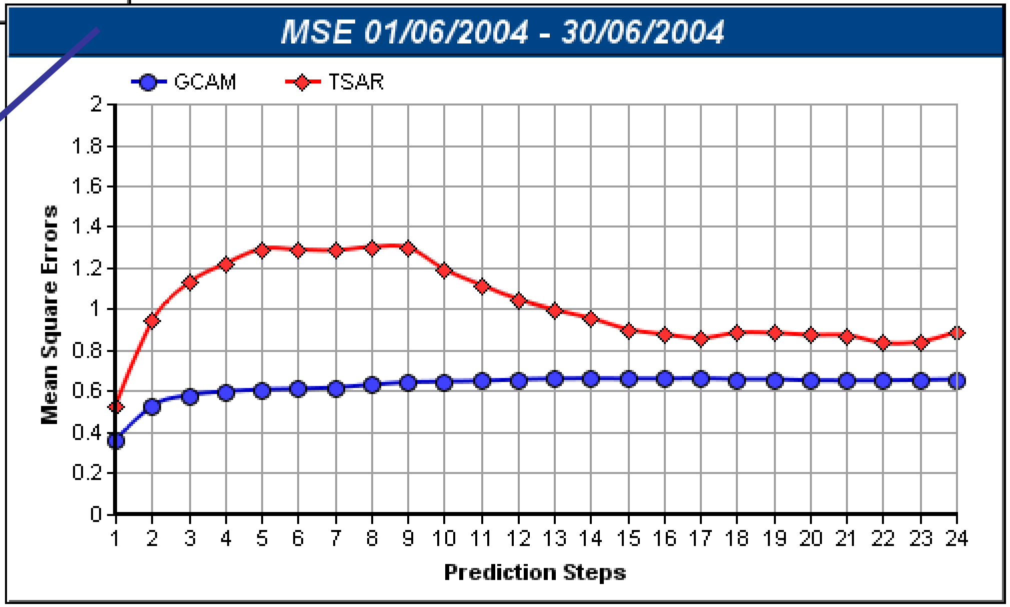

# Ionospheric predictions: "The way ahead"

Use as "driver" the solar wind magnetic field at L1 contributing to the forecast of the high latitude Joule heating at least <u>one hour in advance</u>.

By orbiting the L1 point, ACE will stay in a relatively constant position with respect to the Earth as the Earth revolves around the sun.

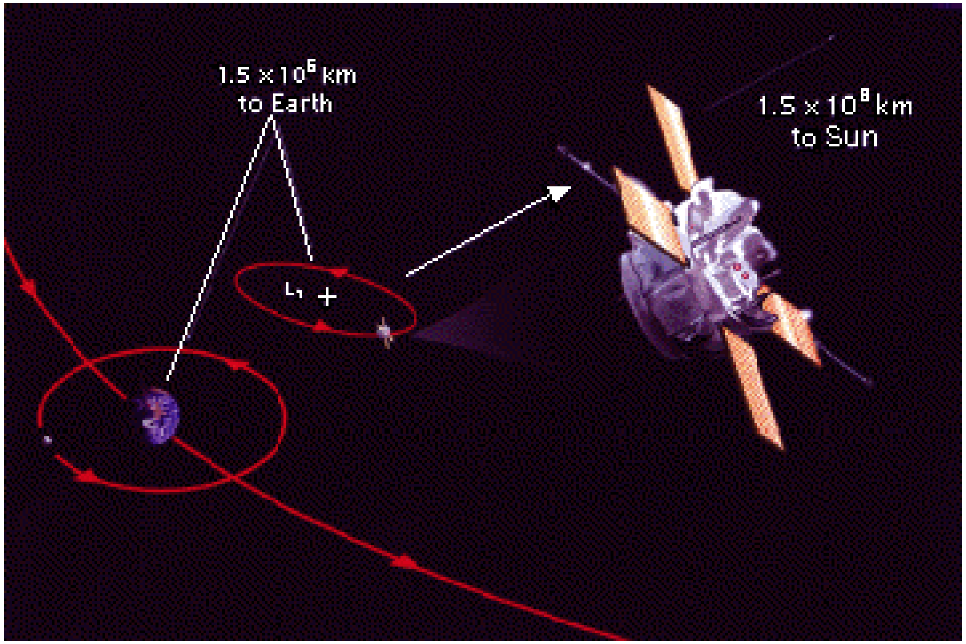

# A real-time dynamic system to specify ionospheric storm effects in middle latitudes

Operational tool developed at RAL (http://ionosphere.rcru.rl.ac.uk) in collaboration with NOA, to study how the IMF parameters are related to subsequent ionospheric disturbances detected at Juliusruh, Chilton, Athens, Rome, Tortosa stations (*Cander, Hickford, Tsagouri and Belehaki, Electronics Letters, 2004*)

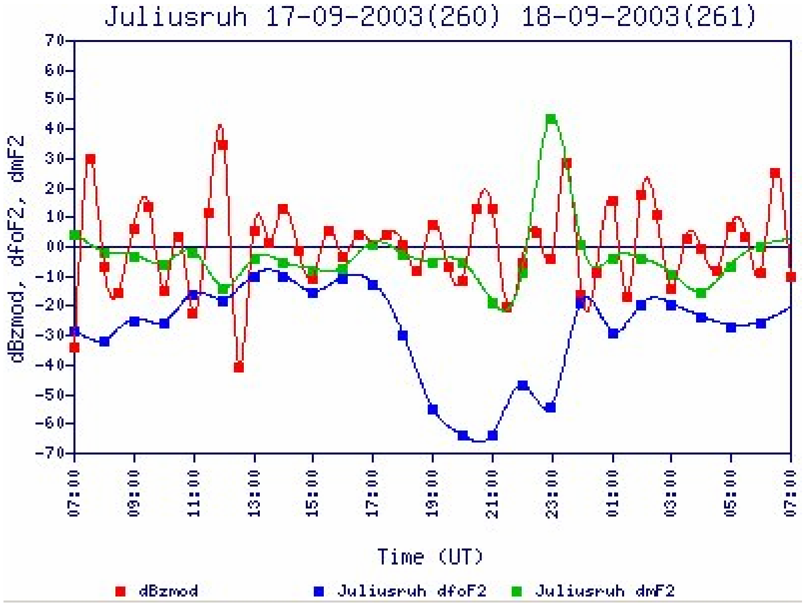


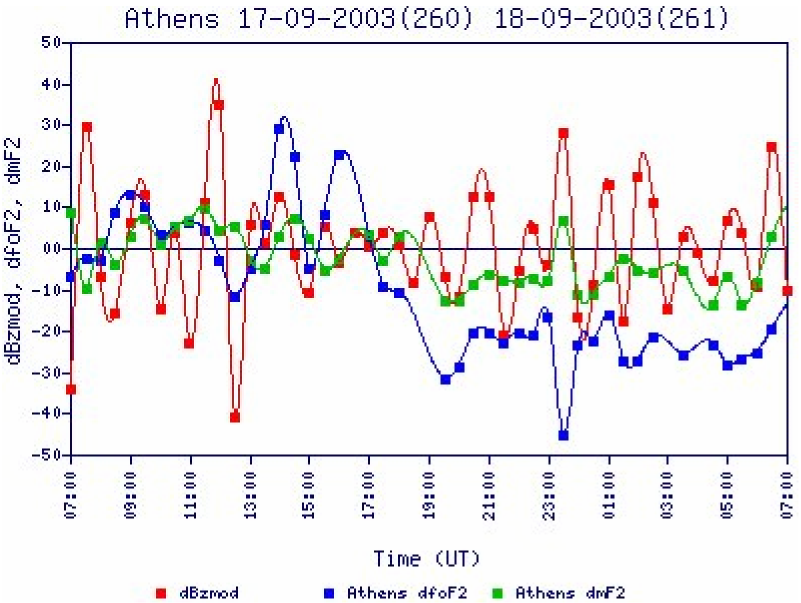

Defining the criteria for issuing alerts for forthcoming ionospheric disturbances is a key issue:

*(after Tsagouri and Belehaki, 2006)*

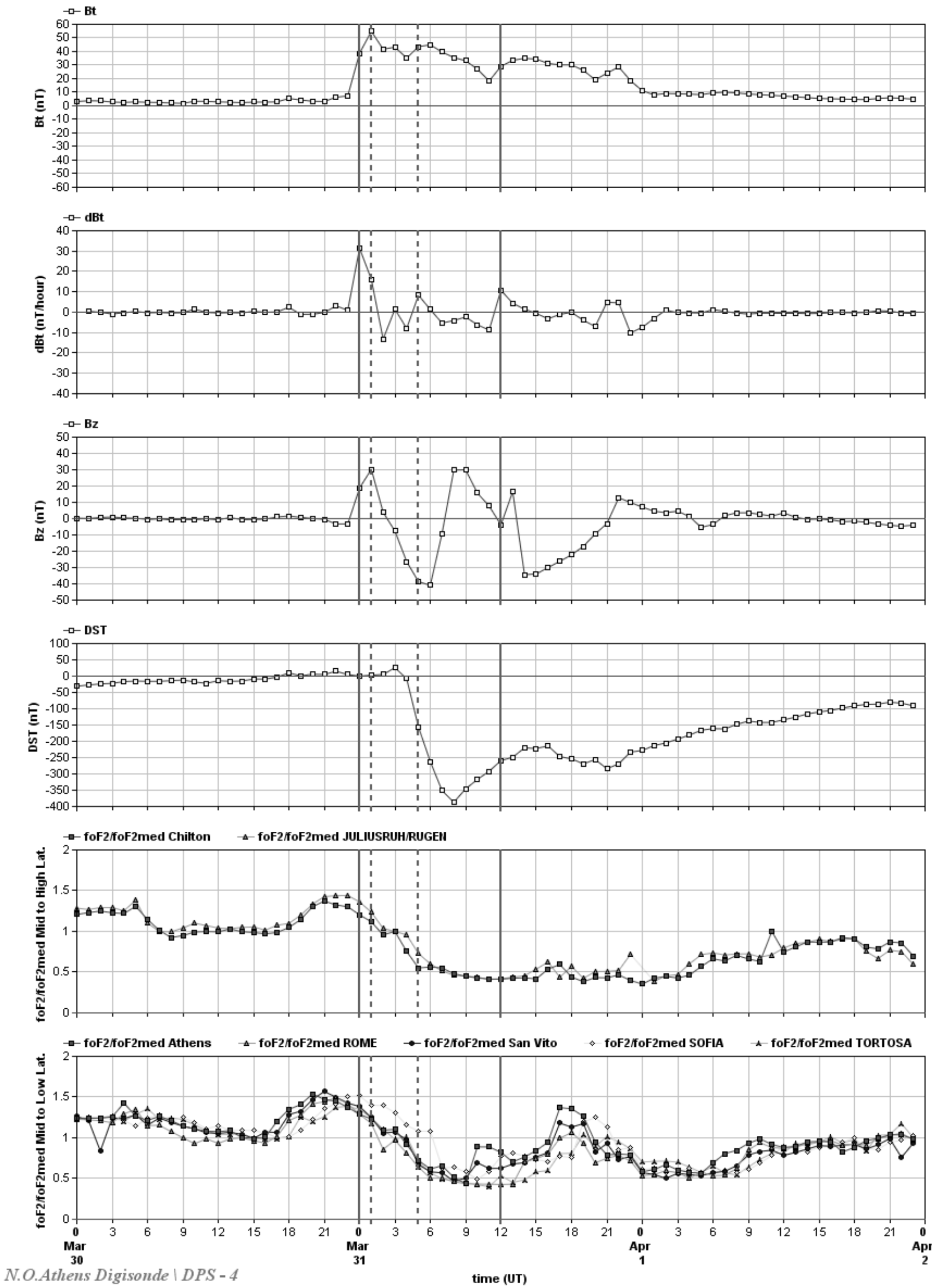

# The superposed epoch analysis results of the ionospheric response in each LT sector *(Tsagouri and Belehaki, ASR 2006)*

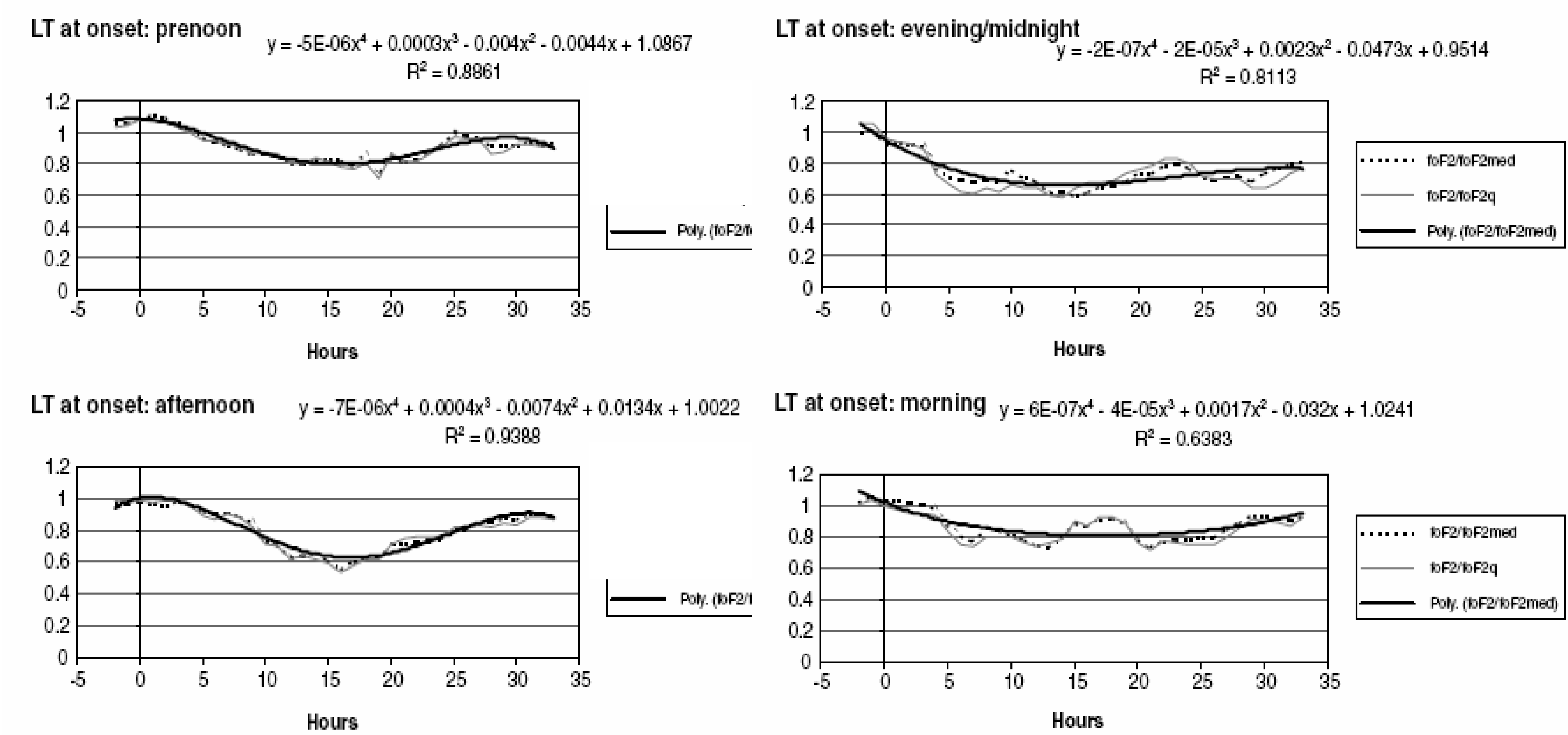

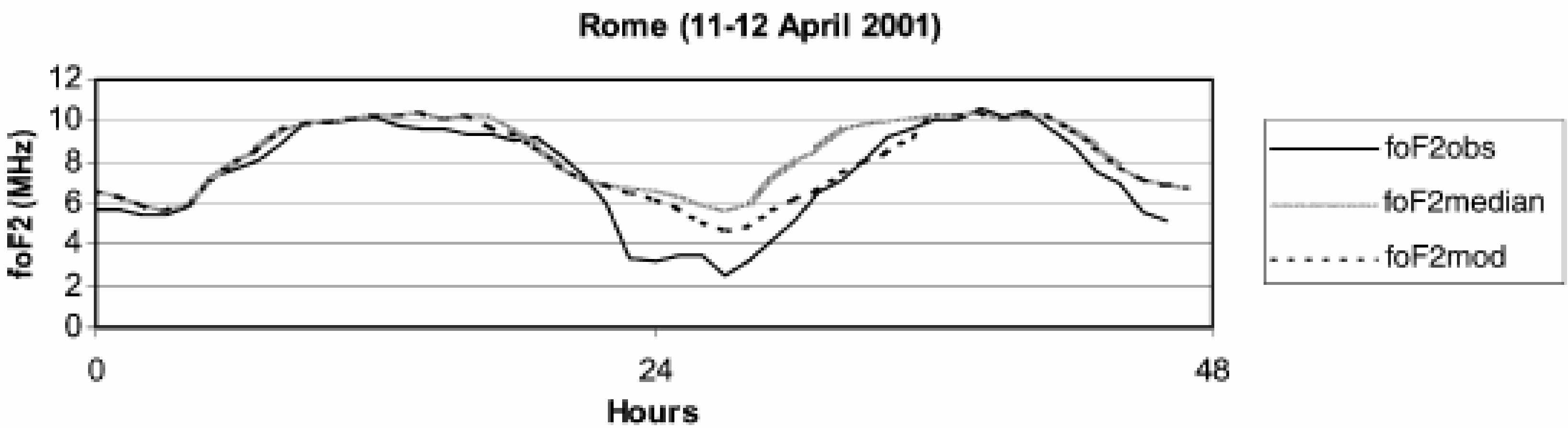


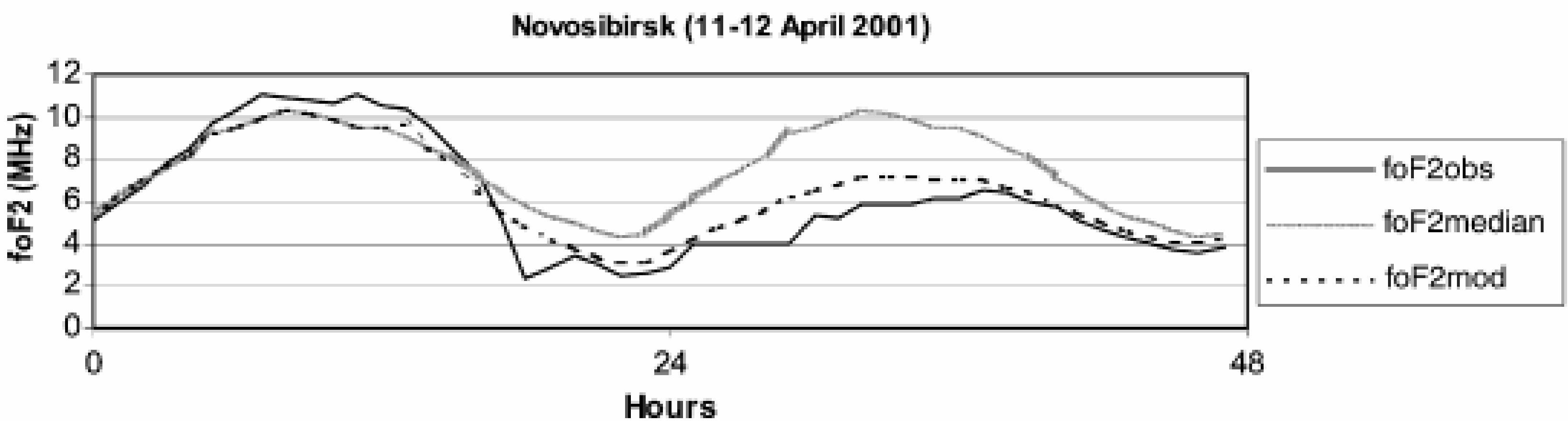


The validation test of the new model (Tsagouri and Belehaki, ASR, 2006) showed an average of 44% improvement on monthly median values during storm days.

# Conclusions

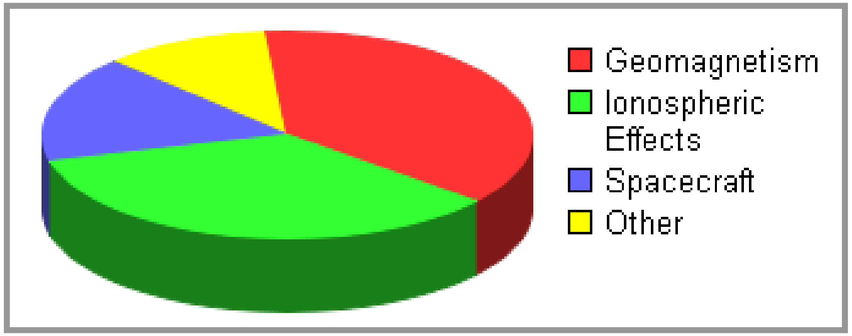


Space Weather Services by type of effects
(ESA GSP Space Weather Pilot Project)

1. Ionospheric space weather effects are among the most important that needed to predicted to serve operational applications.

2. Real-time networks of ground-based sounders are fundamental tools for ionospheric specification and forecasting.

3. Real-time ionospheric models for ionospheric specification and short term ionospheric prediction supported mainly by time series forecasting techniques can be transformed to useful tools for accurate ionospheric prediction using as driver solar wind magnetic field disturbances.